Published for SISSA by Springer

Received: *April 8, 2025*
Revised: *September 18, 2025*
Accepted: *November 2, 2025*
Published: *January 2, 2026*

Searches for power-law warped extra dimensions

Sang Hui Im[a] **and Krzysztof Jodłowski**[a]

[a] *Particle Theory and Cosmology Group, Center for Theoretical Physics of the Universe, Institute for Basic Science (IBS), Daejeon 34126, Republic of Korea*

E-mail: imsanghui@ibs.re.kr, k.jodlowski@ibs.re.kr

Abstract: Extra dimensions with a bulk dilaton field can be power-law warped, unlike the exponential warping in the Randall-Sundrum (RS) model. We show that this mildly warped extra dimension can address the hierarchy problem with a novel Kaluza-Klein (KK) spectrum characterized by lighter feebly coupled KK modes compared to the KK modes in the RS model. We investigate the prospects of searching for signatures of such KK modes at current and future colliders, such as the LHC, CLIC, and FCC-ee using visible decays of KK gravitons. We also update the current bounds and projected limits for the RS model and the linear dilaton (LD) model. Furthermore, we explore the long-lived regime of KK gravitons at beam dump experiments, e.g., FASER2, MATHUSLA, and SHiP, as well as constraints from astrophysical and cosmological observations. We find that combining both kinds of searches will enable comprehensive coverage of the model parameter space relevant to the electroweak hierarchy problem.

Keywords: Extra Dimensions, Specific BSM Phenomenology

ArXiv ePrint: 2412.20913

https://doi.org/10.1007/JHEP01(2026)019

JHEP01(2026)019

Contents

1 Introduction

Extra spatial dimensions beyond the observed 4-dimensional spacetime are an intriguing possibility for physics beyond the Standard Model. String theory requires such extra dimensions for the consistency of the theory, see e.g. [1, 2]. Large flat extra dimensions proposed by Arkani-Hamed, Dimopoulos, Dvali (ADD) [3] and a small warped extra dimension by Randall and Sundrum (RS) [4] have been shown to be able to address the hierarchy problem with predictions on the new particles with observable signatures around the TeV scale. Similarly, a 5D analogue of 7D theory with a linear dilaton background, which provides a dual description of Little String Theories, was proposed to solve the hierarchy problem with distinctive Kaluza-Klein (KK) graviton signatures, which is often referred to as the "linear dilaton model" [5, 6].

Later, an interesting observation was made that the linear dilaton (LD) model can be obtained by taking the continuum limit of the so-called clockwork Lagrangian [7], which was originally introduced to generate hierarchical couplings of a compact field [8–10]. Generalizing this observation, [11] showed that an extra dimension with a bulk dilaton field having a general coupling (hence "*general linear dilaton* (GLD) model") can have more general geometries beyond the ADD model (flat), the RS model (exponentially warped), and the LD model (linearly warped). Using the notation of [11], the metric of this general geometry is given by

$$ds^2 = e^{2k_1 y}\eta_{\mu\nu}dx^\mu dx^\nu + e^{2k_2 y}dy^2, \tag{1.1}$$

where $\mu, \nu = 0, 1, 2, 3$ are 4D spacetime indices, $\eta_{\mu\nu} = \mathrm{diag}(-1, 1, 1, 1)$, y is a coordinate for the extra dimension, and k_1, k_2 are two independent real parameters (but with the same sign)

JHEP01(2026)019

determined by the dilaton potential. By changing the coordinate for the extra dimension from y to z such that $dz = \exp(k_2 y)dy$, this metric is equivalent to

$$ds^2 = (k_2 z + 1)^{2k_1/k_2}\eta_{\mu\nu}dx^\mu dx^\nu + dz^2. \tag{1.2}$$

The previous three well-known extra dimensional models are then identified with $k_1 = 0$ (ADD), $k_1 = k_2$ (LD), and $k_2 \to 0$ (RS). We also note that $k_1/k_2 = 1/6, 1/7$, and $1/10$ are shown to be realized by 5D effective theory of heterotic M-theory [12, 13], and $k_1/k_2 = (N+2)/(N-1)$ by 5D effective theory of $(4+N)$-dimensional spacetime with N compact extra dimensions having a bulk cosmological constant [14].[1]

It was pointed out that LD ($k_1/k_2 = 1$) has a distinctive feature for the KK graviton spectrum characterized by more degenerate masses compared with RS [5–7]. As we will explain in the next section, and also argued in [13], a warped extra dimension with $0 < k_1/k_2 < 1$ can have even more distinctive patterns for KK graviton spectrum and couplings in contrast to the conventional extra dimensional models such as RS and ADD. As naively expected, in this new class of extra dimensions, the KK modes have intermediate features between RS and ADD. Here, let us briefly summarize the characteristics of the KK graviton spectrum and the couplings to the Standard Model (SM) particles for each class of models. The 4D effective Lagrangian for the KK gravitons may be written as

$$\mathcal{S} = \int d^4x \left[-\frac{1}{2}(\partial_\rho h^{(0)}_{\mu\nu})^2 - \frac{h^{(0)}_{\mu\nu}}{M_P}T^{\mu\nu}_{\rm SM} - \sum_{n=1}^{\infty}\left(\frac{1}{2}(\partial_\rho h^{(n)}_{\mu\nu})^2 + \frac{1}{2}m_n^2 (h^{(n)}_{\mu\nu})^2 + C_n \frac{h^{(n)}_{\mu\nu}}{M_5}T^{\mu\nu}_{\rm SM}\right)\right] \tag{1.3}$$

where $h^{(0)}_{\mu\nu}$ is the massless zero mode graviton, $h^{(n)}_{\mu\nu}$ with $n \geq 1$ is the KK graviton with mass m_n and coupling C_n to the energy-momentum tensor $T^{\mu\nu}_{\rm SM}$ of the SM fields, M_P is the 4D reduced Planck mass, and M_5 is the 5D Planck mass, which is around TeV scale in order to address the electroweak hierarchy problem.[2] For each class of models, it can be shown that

$$\begin{aligned}
&\text{RS}: && m_n \sim nk, && C_n \sim \mathcal{O}(1) \\
&\text{LD}: && m_n \sim k\sqrt{1+\left(\frac{n\pi}{\ln(M_P/M_5)}\right)^2}, && C_n \sim \sqrt{\frac{k}{M_5 \ln(M_P/M_5)}}\left[1+\left(\frac{\ln(M_P/M_5)}{n\pi}\right)^2\right]^{-\frac{1}{2}} \\
&\text{ADD}: && m_n \sim nM_5\left(\frac{M_5}{M_P}\right)^2, && C_n \sim \frac{M_5}{M_P} \\
&\text{GLD}: && m_n \sim nk\left(\frac{M_5}{M_P}\sqrt{\frac{M_5}{k}}\right)^{\frac{2(1-k_1/k_2)}{(1+2k_1/k_2)}}, && C_n \sim \frac{M_5}{M_P} n^{\frac{3k_1/k_2}{2(1-k_1/k_2)}}
\end{aligned} \tag{1.4}$$

where $k\,(\lesssim M_5)$ corresponds to the curvature scale of the extra dimension, which can be naturally smaller than M_5 in LD and GLD due to dilaton shift symmetry [6, 7], and we

[1] In ref. [14], the metric is given in the Jordan frame, which is equivalent to the metric (1.1) or (1.2) in the Einstein frame.

[2] Here we take the convention that the IR brane is located at $y = 0$ with the metric (1.1) where the SM particles are localized, while the UV brane is located at $y = \pi R$. Then M_5 is related to M_P by the relation: $M_P^2 \simeq M_5^3 e^{2k\pi R}/k$ where $k = k_1 + k_2/2$.

JHEP01(2026)019

take $0 < k_1/k_2 < 1$ for GLD here. In the case of RS, the KK spectrum and couplings are mostly determined by the scale M_5 ($\sim k$). It is similar in the case of LD if the curvature k is comparable to M_5, except for the feature that the KK spectrum is more compressed. On the contrary, the KK modes of ADD are much lighter than M_5, and their couplings are as small as the zero mode graviton coupling, which is suppressed by the 4D Planck scale. On the other hand, the KK gravitons of a power-law warped extra dimension with $0 < k_1/k_2 < 1$ can be parametrically lighter than M_5, similar to ADD, while having sizable couplings larger than the zero mode graviton coupling for large n.

The pattern of the KK spectrum and couplings of GLD with $0 < k_1/k_2 < 1$ is thus similar to ADD for lightest KK states, while it shows substantial difference for heavy KK states with large n characterized by sizable couplings that may allow larger production of the heavy KK states at colliders. The ADD model with one extra dimension is heavily constrained by astrophysical processes, in particular the Supernova 1987A (SN1987), which require $M_5 \gtrsim 700\,\text{TeV}$ [15], and therefore cannot provide a *natural* solution to the hierarchy problem. On the other hand, the phenomenology of GLD with $0 < k_1/k_2 < 1$ has not been comprehensively studied before, while it can be realized in some concrete UV setups, e.g. heterotic string theory [12, 13]. In this work, we found that GLD with $k_1/k_2 \gtrsim 1/3$ can provide a solution to the hierarchy problem with the natural Higgs mass scale $\sim M_5$ less than 10 TeV with some predictions on KK graviton signatures in future colliders and relatively weak constraints from astrophysical objects, while GLD with $0 < k_1/k_2 \lesssim 1/3$ is rather strongly constrained by astrophysical bounds on M_5.

Another interesting point for LD and GLD phenomenology is that the curvature k of the extra dimension can be parametrically smaller than M_5 thanks to the dilaton shift symmetry, as discussed in [6, 7]. The curvature k breaks the translation invariance, allowing decays of heavier gravitons to lighter ones, which do not happen in ADD, because the decay would happen at threshold [3], where phase space vanishes. The decay branching ratios into lighter KK states turn out to be negligible, unless the mass ratio of the decaying KK particle to a lighter KK particle is sufficiently large. Such a large mass ratio can be naturally obtained in LD with a small $k \ll M_5$ or in GLD with $0 < k_1/k_2 < 1$. As a result, in the low curvature region of LD, $k \ll M_5$, it was claimed that the SM signatures at the LHC are suppressed because the heavier KK states decay into lighter ones with significant branching ratios, while the lighter states are long-lived and escape the LHC detectors [7, 16, 17]. We re-examined this issue and found that such inner KK tower decays are actually negligible even for small k in LD and more generally for $k_1/k_2 \gtrsim 1/2$ in GLD. On the other hand, such long-lived regime with small $k \ll M_5$ can be covered by present and future electron or proton beam dump experiments, see [18] for a recent review, which look for, e.g., $\sim$ GeV mediators between the SM and the dark sector such as axion-like particles (ALPs), dark photon, dark Higgs, or sterile neutrinos, among others. We will show that in addition to collider searches, beam dumps can also be effective in constraining extra dimensional theories by looking for visible decays of KK states.

This paper is organized as follows. In section 2, we discuss power-law warped extra dimensions originating from GLD, in particular the spectrum and couplings of the KK gravitons, which are crucial for phenomenology. In section 3, we discuss the signatures of the KK gravitons from RS, LD, and GLD at the LHC, upcoming lepton colliders, beam dumps,

JHEP01(2026)019

and astrophysical processes. In section 4, we present and discuss our results — the main ones being sensitivity plots of these experiments and observations. We also discuss the importance of KK graviton decays into lighter KK states. In particular, we find the LHC searches for the LD are stronger than the previous results in ref. [6] in the $k \ll M_5$ region. We conclude in section 5, while auxiliary sections are in the appendix. In appendix A, we present the derivation of the GLD solution. In appendix B, we succinctly recall the astrophysical bounds on flat large extra dimensions, and we present the revised (weaker) limits. Technical details of our analysis are relegated to appendix C.

2 Power-law warped extra dimensions

In this section, we will show that an extra dimension with a general warping in eq. (1.2) can be realized by a bulk dilaton field background. Subsequently, we will discuss the spectrum and couplings of the KK gravitons relevant for our phenomenological analysis. The discussion will closely follow refs. [11, 13].

2.1 General linear dilaton model

The GLD model introduced in [11] may be defined as the following 5D action in the Jordan frame:

$$\mathcal{S} = \int d^4x \int_{-\pi R}^{\pi R} dy \sqrt{-g}\, e^{\xi S} \left(\frac{M_5^3}{2} R_5 + \frac{M_5^3}{2} \partial^M S \partial_M S - \Lambda_5 - \frac{1}{\sqrt{g_{55}}} [\Lambda_0 \delta(y) + \Lambda_\pi \delta(y - \pi R)] \right), \tag{2.1}$$

where the extra dimension is described by the coordinate $y \in [-\pi R, \pi R]$ and orbifolded with Z_2-identification $y \equiv -y$, M_5 is the 5D Planck mass, Λ_5 is the bulk constant parameter, Λ_0 and Λ_π are the tensions of 3-branes localized at $y = 0$ and $y = \pi R$, respectively, and R_5 is the 5D Ricci scalar. S is the dilaton field propagating over the extra dimension, and interactions involving the dilaton field are determined by the overall factor $e^{\xi S}$ in the Jordan frame with a real coupling constant ξ. This form of dilaton interactions may be motivated by the *classical scale invariance* of effective actions originating from string theory [19, 20]. It requires that classical equations of motion of the action $\mathcal{S}$ do not change under the scale transformation realized by dilaton shift symmetry $S \to S + \alpha$ in the Jordan frame. For further discussion of this point, we refer the readers to section 2.2 of [6].

The action (2.1) can be written in the Einstein frame by redefining the metric as

$$g_{MN} \to e^{-2\xi S/3} g_{MN}, \tag{2.2}$$

where Latin letters stand for 5D spacetime indices $M, N = 0, 1, 2, 3, 5$. Furthermore, setting the canonical normalization of the dilaton field, the action becomes

$$\begin{aligned} \mathcal{S} = \int d^4x \int_{-\pi R}^{\pi R} dy \sqrt{-g} \Bigg(& \frac{M_5^3}{2} R_5 - \frac{M_5^3}{2} \partial^M S \partial_M S - e^{-2\lambda S/\sqrt{3}} \Lambda_5 \\ & - \frac{e^{-\lambda S/\sqrt{3}}}{\sqrt{g_{55}}} [\Lambda_0 \delta(y) + \Lambda_\pi \delta(y - \pi R)] \Bigg), \end{aligned} \tag{2.3}$$

JHEP01(2026)019

where the dilaton coupling λ in the Einstein frame is given by

$$\lambda = \frac{\xi}{\sqrt{4\xi^2 - 3}}. \tag{2.4}$$

Here we note that it is needed that

$$\xi^2 > \frac{3}{4} \tag{2.5}$$

in order for the dilaton S not to be a ghost field in the Einstein frame. It will turn out to be convenient to use parametrization

$$\Lambda_5 = -2M_5^3 k_b^2, \quad \Lambda_0 = -4M_5^3 k_0, \quad \Lambda_\pi = -4M_5^3 k_\pi. \tag{2.6}$$

As discussed in [6, 7], we remark that the shift symmetry $S \to S + \alpha$ in the Einstein frame is restored in the bulk as $k_b \to 0$. Therefore, small $k_b \ll M_5$ is technically natural in GLD models — contrary to RS, where the dilaton is decoupled — and we will examine its phenomenological consequences in subsequent sections.

A solution to the equations of motion for the metric field g_{MN} and the dilaton field S of the action (2.3) is given in [11]; it is also derived in appendix A. It is

$$ds^2 = e^{2k_1|y|}(\eta_{\mu\nu}dx^\mu dx^\nu) + e^{2k_2|y|}dy^2, \quad \frac{\lambda}{\sqrt{3}}S = k_2|y| + \frac{\lambda}{\sqrt{3}}S_0\,, \tag{2.7}$$

where Greek letters stand for 4D spacetime indices $\mu, \nu = 0, 1, 2, 3$,

$$k_1 = \frac{2k_b}{\sqrt{3(4-\lambda^2)}}e^{-\lambda S_0/\sqrt{3}}, \quad k_2 = \lambda^2 k_1\,, \tag{2.8}$$

and S_0 is the vacuum expectation value of S at $y = 0$ which can be determined by an additional brane potential for S as demonstrated in [6]. Also the brane tension terms Λ_0 and Λ_π have to satisfy

$$k_0 e^{-\lambda S_0/\sqrt{3}} = -k_\pi e^{-\lambda S_0/\sqrt{3}} = \frac{3}{2}k_1 \tag{2.9}$$

in order to have the 4D Minkowski background. In eq. (2.7), the dilaton field solution is linear in the extra dimensional coordinate, i.e. $S \propto y$. This is the reason why this model is often called *linear dilaton* model. Also, it is *general* linear dilaton model, since the general dilaton coupling ξ is introduced, while $\xi = 1$ in the original linear dilaton model studied in [5, 6].

Therefore, the metric solution in eq. (2.7) with the linear dilaton background realizes a generally warped extra dimension, for which the metric can be rewritten as eq. (1.2) by changing the extra dimensional coordinate from y to z such that $dz = e^{k_2|y|}d|y|$:

$$ds^2 = (k_2 z + 1)^{2k_1/k_2}\eta_{\mu\nu}dx^\mu dx^\nu + dz^2\,, \tag{2.10}$$

where $z \in [0, (e^{k_2\pi R} - 1)/k_2]$ and

$$\frac{k_1}{k_2} = 4 - \frac{3}{\xi^2}\,, \tag{2.11}$$

$$k_2 = \frac{2\xi^2}{3(4\xi^2 - 3)}\sqrt{\frac{4\xi^2 - 3}{5\xi^2 - 4}}k_b e^{-\lambda S_0/\sqrt{3}}\,. \tag{2.12}$$

Thus, the dilaton coupling ξ in the Jordan frame action (2.1) determines the power ($= k_1/k_2$) of the warping, while the bulk constant parameter $\Lambda_5 = -2M_5^3 k_b^2$ and the dilaton vacuum value S_0 at $y = 0$ controls the curvature factor k_2. Moreover, Eq. (2.11) tells us that $k_1/k_2 > 0$ from the ghost-free condition (2.5), which means that k_1 and k_2 must have the same sign.

2.2 Spectrum and couplings of Kaluza-Klein gravitons

The KK gravitons arise from the tensor fluctuation $h_{\mu\nu}(x, y)$ of the 4D part of the metric on the background given by eq. (2.7):

$$ds^2 = e^{2k_1|y|}(\eta_{\mu\nu} + 2h_{\mu\nu}(x, y))dx^\mu dx^\nu + e^{2k_2|y|}dy^2. \tag{2.13}$$

The effective action for the 4D metric fluctuation can be found by inserting the above metric to the action (2.3). Working in the traceless-transverse gauge, $h^\mu_\mu = \partial^\mu h_{\mu\nu} = 0$, the action for the fluctuation to quadratic order in $h_{\mu\nu}$ is

$$\mathcal{S}_h = -M_5^3 \int d^4x \int_{-\pi R}^{\pi R} dy\, e^{(2k_1+k_2)|y|} \left[\frac{1}{2}(\partial_\rho h_{\mu\nu})^2 + \frac{1}{2}e^{2(k_1-k_2)|y|}(\partial_y h_{\mu\nu})^2\right]. \tag{2.14}$$

The equation of motion for the graviton field $h_{\mu\nu}(x, y)$ from the above action comes out as

$$\partial_y^2 h_{\mu\nu} + 2(k + p)\epsilon(y)\partial_y h_{\mu\nu} + e^{-2p|y|}\eta^{\rho\sigma}\partial_\rho\partial_\sigma h_{\mu\nu} = 0\,, \tag{2.15}$$

where $\epsilon(y) \equiv \partial_y|y|$, and

$$\begin{aligned} k &\equiv k_1 + \frac{k_2}{2}\,, \\ p &\equiv k_1 - k_2\,. \end{aligned} \tag{2.16}$$

To find a solution to eq. (2.15), let us decompose $h_{\mu\nu}(x, y)$ as

$$h_{\mu\nu}(x, y) = \sum_{n=0}^{\infty} h_{\mu\nu}^{(n)}(x)h_n(y)\,, \tag{2.17}$$

where we assume that $h_{\mu\nu}^{(n)}(x)$ is a 4D mass eigenstate with mass m_n,

$$\eta^{\rho\sigma}\partial_\rho\partial_\sigma h_{\mu\nu}^{(n)}(x) = m_n^2 h_{\mu\nu}^{(n)}(x). \tag{2.18}$$

Using eq. (2.18), the equation of motion (2.15) implies

$$\partial_y^2 h_n(y) + 2(k + p)\epsilon(y)\partial_y h_n(y) + e^{-2p|y|}m_n^2 h_n(y) = 0. \tag{2.19}$$

The solutions to eq. (2.19) for $p \neq 0$ turn out to be given by Bessel functions:

$$h_0(y) = \frac{1}{N_0} \text{ with } m_0 = 0, \tag{2.20}$$

$$h_n(y) = \frac{1}{N_n}e^{-(k+p)|y|}\left[J_\alpha\left(\frac{m_n}{|p|}e^{-p|y|}\right) + c_n Y_\alpha\left(\frac{m_n}{|p|}e^{-p|y|}\right)\right] \text{ with } m_n \neq 0, \tag{2.21}$$

where N_n is a normalization factor, $\alpha = 1 + k/p$, J_α and Y_α are the Bessel functions of the first kind and the second kind, respectively. The coefficient c_n is determined by the following boundary values of the Bessel functions, in order to satisfy eq. (2.19):

$$c_n = -\frac{J_{\alpha-1}\left(\frac{m_n}{|p|}\right)}{Y_{\alpha-1}\left(\frac{m_n}{|p|}\right)} = -\frac{J_{\alpha-1}\left(\frac{m_n}{|p|}e^{-p\pi R}\right)}{Y_{\alpha-1}\left(\frac{m_n}{|p|}e^{-p\pi R}\right)}\,. \tag{2.22}$$

For the special case $p = 0$, the solutions to eq. (2.19) are given by

$$h_0(y) = \frac{1}{N_0} \text{ with } m_0 = 0, \tag{2.23}$$

$$h_n(y) = \frac{1}{N_n}e^{-k|y|}\left[k\sin\left(\frac{n}{R}|y|\right) + \frac{n}{R}\cos\left(\frac{n}{R}|y|\right)\right] \text{ with } m_n \neq 0, \tag{2.24}$$

where n is a positive integer. This special case corresponds to the original linear dilaton model given in [5, 6], which is defined by $\xi = 1$ in eq. (2.1).

Eq. (2.22) and the solution (2.24) determine the mass eigenvalue m_n of the KK graviton mode $h^{(n)}_{\mu\nu}(x)$ as

$$m_n \begin{cases} \simeq \left(n - \frac{1}{4} + \left|\frac{k}{2p}\right|\right)\pi p\,, & p > 0 \\ = \sqrt{k^2 + \frac{n^2}{R^2}}\,, & p = 0 \\ \simeq \left(n - \frac{1}{4} + \left|\frac{k}{2p}\right|\right)\pi|p|e^{-|p|\pi R}\,, & p < 0 \end{cases} \tag{2.25}$$

where $n > 1/4 - |k/2p|$ is an integer for $p \neq 0$ and a positive integer for $p = 0$.

Let us now discuss couplings of the KK gravitons to the SM particles. We assume that the SM particles are localized on the brane located at $y = 0$, and we take $k_2 = \lambda^2 k_1 > 0$ in order to address the hierarchy problem. The KK gravitons couple to the brane-localized SM Lagrangian $\mathcal{L}_{\rm SM}$ by the interaction

$$\mathcal{S}_{\rm int} = \int d^4x \int_{-\pi R}^{\pi R} dy\sqrt{-g}\,\frac{1}{\sqrt{g_{55}}}\delta(y)\mathcal{L}_{\rm SM}\,, \tag{2.26}$$

which gives rise to

$$\mathcal{S}_{\rm int} = \int d^4x \left[\mathcal{L}_{\rm SM} - h_{\mu\nu}(x,0)T^{\mu\nu}_{\rm SM} + \mathcal{O}(h^2_{\mu\nu})\right], \tag{2.27}$$

where

$$T^{\mu\nu}_{\rm SM} = -2\frac{\partial\mathcal{L}_{\rm SM}}{\partial g_{\mu\nu}} + g^{\mu\nu}\mathcal{L}_{\rm SM}\Big|_{g_{\mu\nu}=\eta_{\mu\nu}}\,. \tag{2.28}$$

After integrating out the extra dimension from eq. (2.14) and using eq. (2.27) for interaction terms, the 4D effective action for the massless graviton and the KK gravitons in the Minkowski background comes out as

$$\mathcal{S} = \int d^4x \left[-\frac{1}{2}(\partial_\rho h^{(0)}_{\mu\nu})^2 - \frac{h^{(0)}_{\mu\nu}}{M_P}T^{\mu\nu}_{\rm SM} - \sum_{n=1}^{\infty}\left(\frac{1}{2}(\partial_\rho h^{(n)}_{\mu\nu})^2 + \frac{1}{2}m_n^2(h^{(n)}_{\mu\nu})^2 + C_n\frac{h^{(n)}_{\mu\nu}}{M_5}T^{\mu\nu}_{\rm SM}\right)\right], \tag{2.29}$$

where m_n is given in eq. (2.25), and[3]

$$M_P = \sqrt{\frac{M_5^3}{k}(e^{2k\pi R} - 1)}, \tag{2.30}$$

$$C_n \begin{cases} \simeq (-1)^{n-1}\sqrt{\frac{p}{M_5}}, & p > 0 \\ = \frac{1}{\sqrt{M_5 \pi R}} \frac{n}{\sqrt{k^2R^2+n^2}}, & p = 0 \\ \simeq \sqrt{\frac{\pi|p|}{M_5}} \frac{e^{-k\pi R}}{\Gamma(k/|p|)} \left[\frac{\pi}{2}\left(n - \frac{1}{4} + \left|\frac{k}{2p}\right|\right)\right]^{\frac{k}{|p|}-\frac{1}{2}}, & p < 0\,. \end{cases} \tag{2.31}$$

Eq. (2.30) shows that the 5D Planck scale M_5 can be exponentially smaller than the 4D Planck scale M_P, which provides a solution to the electroweak hierarchy problem if M_5 is around the electroweak scale. This exponential hierarchy $\sim e^{(k_1+k_2/2)\pi R}$ between M_5 and M_P stems from two factors: a large extra dimension with size $L \sim e^{k_2\pi R}/k_2$ and the power-law warping $(k_2 L)^{k_1/k_2} \sim e^{k_1\pi R}$ as can be seen from the metric (2.10). Therefore, GLD with $k_2 \neq 0$ including LD addresses the hierarchy problem by both a large extra dimension (as ADD) and a warp factor (as RS).

The masses and couplings of the KK gravitons in GLD with $p < 0$ show a particularly different parametric behavior compared to the conventional models such as ADD, RS, and LD. Taking $k \sim p \sim M_5$ for simplicity, eq. (2.25) and eq. (2.31) shows that $m_n \sim nM_5$ and $C_n \lesssim \mathcal{O}(1)$ for $p \geq 0$ as in RS and LD. On the other hand, for $p < 0$, the KK graviton masses are $m_n \sim nM_5(M_5/M_P)^{|p|/k}$ as in ADD with $2k/|p|$ flat extra dimensions, but the KK graviton couplings are $C_n \sim (M_5/M_P) \times n^{(k/|p|-1/2)}$ which is clearly different from ADD where $C_n = M_5/M_P$. This difference can be significant for heavy KK states with large n. As we will show in section 4, this feature allows better sensitivity on M_5 at future colliders such as CLIC compared to ADD models due to larger cross section for heavy KK states.

3 Signatures of extra dimensions

In this section, we present the observable characteristics of RS, LD, and GLD models, which will be further investigated in present and future experiments, as well as in astrophysical observations. In fact, phenomenology of a KK graviton crucially depends on its mass and coupling strength, which *uniquely* determines both its lifetime and branching ratios — the 4D effective Lagrangian in eq. (2.29) has the same coupling strength to all SM fields.[4] Since the KK graviton G_n couples to SM states through the mass dimension-5 operator, its decay width has the form $\Gamma_{G_n} \sim m_{G_n}^3/\Lambda_n^2$ with $\Lambda_n \equiv M_5/C_n$ as can be seen in eq. (2.29). In figure 1 and figure 2, we present the dependence of the lifetime and branching ratios of a KK graviton as a function of its mass, respectively. In figure 1, on the left, we show the lifetime of the KK graviton in RS ($\lambda^2 = 0$) and LD ($\lambda^2 = 1$) in terms of m_{G_n} and Λ_n, which can be taken to be approximately independent of each other in RS and LD. On the other

[3]For $p < 0$, C_n for $m_n \gg |p|$ is bounded above by $\sim \sqrt{|p|/M_5}e^{-\frac{1}{2}|p|\pi R}$.

[4]If any of the couplings to the SM states were different from each other, perturbative unitarity would be violated due to the non-decoupling of the helicity zero or one states [21]; see [22] for an explicit computation of $e^+e^- \to G_n\gamma$ process, which illustrates the general phenomena. In fact, the Ward identity for a massive spin-2 state is equivalent to conservation of energy-momentum tensor.

JHEP01(2026)019

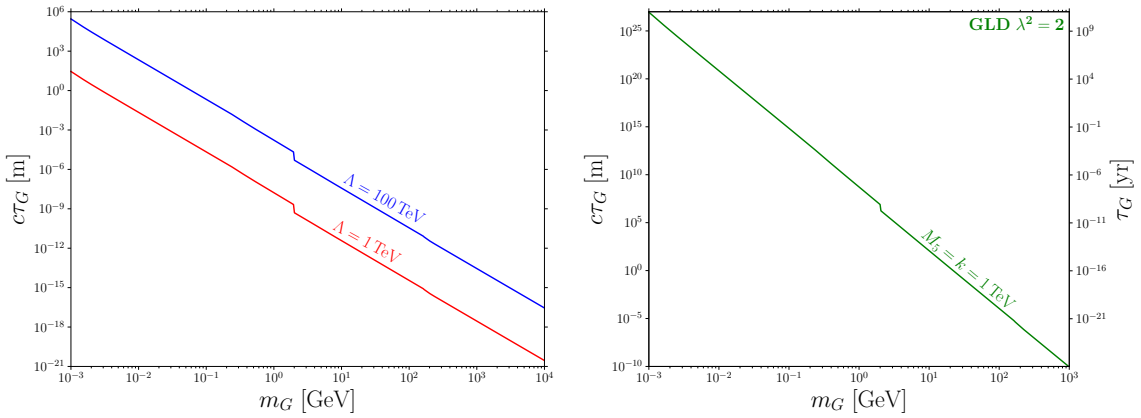

Figure 1. Lifetime of KK gravitons, expressed in meters, as a function of their masses for several benchmarks of GLD model. The left panel presents the result for RS ($\lambda = 0$) and LD ($\lambda = 1$), while the right one — for $\lambda^2 = 2$ and fixed values of curvature and 5D Planck mass, $k = M_5 = 1\,\mathrm{TeV}$. In the left panel, the red and blue lines correspond to fixed values of the 4D coupling $\Lambda = 1\,\mathrm{TeV}$ and $\Lambda = 100\,\mathrm{TeV}$, respectively, ($\Lambda \equiv M_5/C_n$, see eq. (2.29)) that can be probed at current and future searches we consider — cf. figure 3. For $\lambda^2 > 1$, the KK graviton coupling to SM is suppressed by $\Lambda \sim M_P$ for the lightest KK graviton, while heavier states have larger couplings proportional to a power of KK graviton mass (e.g. $\Lambda \sim 10^7\,\mathrm{GeV}$ for $m_G \sim 1\,\mathrm{TeV}$ in the GLD model with $\lambda^2 = 2$).

hand, for GLD models with $\lambda^2 > 1$, the coupling $1/\Lambda_n$ heavily depends on the mass m_{G_n}. Therefore, on the right of figure 1, we show the lifetime of KK graviton for GLD models with $\lambda^2 > 1$ in terms of m_{G_n} and M_5, taking the curvature $k = M_5$ and a benchmark point $\lambda^2 = 2$. The plots show that KK gravitons of masses between MeV and TeV exhibit a wide range of lifetimes, spanning both short-lived regime ($c\tau_G \lesssim 1$ m) and long-lived regime ($c\tau_G \gtrsim 1$ m). Comparing the plots, one can also see that GLD with $\lambda^2 > 1$ has much more long-lived KK gravitons compared with RS and LD.

Figure 2 illustrates that while low-mass KK gravitons decay into photons and neutrinos with $1 : 3/4$ ratio,[5] hadronic states dominate for heavier states. Also, KK gravitons can invisibly decay into neutrinos and lighter KK gravitons. If $\lambda^2 \lesssim 2$, however, the decay branching ratio into lighter KK gravitons turns out to be negligible. On the other hand, the inner KK tower decays become significant for $\lambda^2 \gtrsim 2$, and so KK gravitons mostly decay into the lightest gravitons invisibly. We will explain this point in more details in section 4 as we discuss astrophysical implications of such inner KK tower decays. Since the dominant decay channels of KK gravitons typically involve SM states for $\lambda^2 \lesssim 2$, we examine their visible decays in two distinct regimes: short-lived, with decay lengths below $1\,m$, and long-lived, with decay lengths exceeding $1\,m$. The former regime is relevant to collider searches, while the latter is pertinent to beam dump experiments, astrophysical, and cosmological observations. Since these two regimes are characterized by different physical features, combining the two allows for an effective coverage of a large part of the parameter space.

[5]We assumed Majorana neutrinos; for Dirac neutrinos, the ratio is $1 : 3/8$.

JHEP01(2026)019

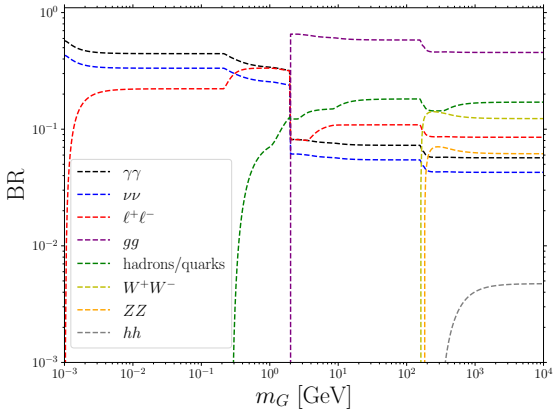

Figure 2. Branching ratios of KK graviton decay as a function of mass. The shown branching ratios hold universally for all GLD models with $\lambda^2 \lesssim 2$. For GLD models with larger λ^2, the inner KK tower decays ($G_n \to G_k G_l$) can be dominant with some implications in astrophysical processes, which we discuss in section 4.

3.1 Short-lived regime

In this regime KK gravitons decay with decay lengths of $d \lesssim 1\,m$. They can be searched at the LHC [6, 23, 24] or at the upcoming e^+e^- colliders like Future Circular Collider (FCC-ee) [25] and Compact Linear Collider (CLIC) [26]. Since the branching ratios of decays into a pair of photons or leptons may be sizable, and constitute a clean experimental channel, we will mainly focus on them. Moreover, a lepton version of the FCC, is planned to be constructed before hadron collider. On the other hand, in section 4, we will also present results for KK gravitons decaying into any visible SM states, mainly into heavy quarks and gluons, which constitute the majority of the decay widths.

The LHC. At the LHC, the n-th KK graviton can be produced by gluon fusion or through interactions with quarks. The total cross section is given by [6]

$$\sigma_n = \frac{\pi}{48\Lambda_n^2}\left(3\mathcal{L}_{gg}(\hat{m}_n^2) + 4\sum_q \mathcal{L}_{qq}(\hat{m}_n^2)\right), \tag{3.1}$$

where $1/\Lambda_n = C_n/M_5$ is the KK graviton coupling to the SM fields as given in eq. (2.31), q are quark fields, $\mathcal{L}(\hat{s})$ are parton luminosities,

$$\mathcal{L}(\hat{s}) = \frac{\hat{s}}{s}\int_{\frac{\hat{s}}{s}}^1 \frac{dx}{x} f(x) f\left(\frac{\hat{s}}{xs}\right), \tag{3.2}$$

where $s = 13\,\text{TeV}$, and $f(x)$ are the parton distribution functions (PDFs). In our analysis, we use the LHAPDF6 library [27–29], which incorporates state-of-the-art PDFs, reflecting the latest experimental data and theoretical advancements. Since the gluon luminosity dominates at high energies, $gg \to G_n$ is the primary production mechanism for KK gravitons. Note that G_n production together with a SM particle in final state, for example quark or gluon, is suppressed by $\sim \alpha_s/(8\pi)$. Therefore, the number of di-photon events is given

JHEP01(2026)019

by the expression:

$$N = \mathcal{L} \times \sum_n \sigma_n \times \mathrm{BR}(G_n \to \gamma\gamma), \tag{3.3}$$

where we sum over the KK graviton modes decaying inside the ATLAS/CMS detectors. In order to determine the exclusion limits from the LHC, we follow the discussion and data from [6, 16, 17, 30]. The exclusion limits are established by comparing the predicted number of di-photon events to the observed data from the ATLAS and CMS experiments. In particular, we impose the cut on the diphoton invariant mass, $m_{\gamma\gamma} > 2.24\,\mathrm{TeV}$, which leads to the most stringent limits [31].

Let us note that other searches (for example, due to resonant searches of di-lepton) at the LHC result in weaker bounds. In particular, one would expect that due to suppression of the di-photon decay — see figure 2 — the hadronic decays of G_n would lead to stronger bounds. However, as is well-known for ADD [24] and LD [30], the shape and the normalization of jet distribution suffer from large uncertainties. As a result, the dijet search, originating from hadronic decays of G_n produced in gluon fusion, leads to subdominant bounds in all considered benchmarks of GLD. Finally, following refs. [32, 33], we found that displaced decay searches at the LHC, which cover the regime $d = c\tau\gamma\beta \sim 1\,m$, do not yield competitive limits. This occurs because efficiently produced KK gravitons decay promptly, whereas the long-lived regime corresponds to the suppressed tail of the production cross-section distribution, resulting in insufficient event rates for detection.

Electron-positron colliders. At the lepton colliders, we calculate the production cross section of KK gravitons in association with a photon or Z boson, $e^+e^- \to G\gamma$ and $e^+e^- \to GZ$, respectively.[6] For the former process, we use results from [34, 35], while for the latter process, we calculated the averaged amplitude squared, given by eq. (C.1).

Specifically we will consider two future lepton colliders, FCC and CLIC, primarily motivated by their different center-of-mass energies. The former allows producing unprecedentedly large number of Z bosons with center-of-mass energy of $\mathcal{O}(100)\,\mathrm{GeV}$, while the linear CLIC allows multi-TeV energy with relatively less luminosity. As we will see in section 4, CLIC produces highly boosted KK gravitons that decay outside the detector in the small k region, limiting its coverage of this parameter space, whereas FCC can effectively probe this region of parameter space.

The number of decays is given by luminosity multiplied by the total production cross section and the branching ratios into the relevant SM states (mainly a pair of photons or leptons):

$$N = \mathcal{L} \times \sum_n \sigma\left(e^+e^- \to XG_n\right) \times \mathrm{BR}_n. \tag{3.4}$$

The effective production cross section is given by

$$\sigma\left(e^+e^- \to XG_n\right) = \int d\Omega\, \frac{d\sigma\left(e^+e^- \to GX\right)}{d\Omega} \left(1 - e^{-R/L_G^{\perp}(\theta)}\right), \tag{3.5}$$

[6] We also took into account the resonant production $e^+e^- \to G$, which we found to be subdominant, see eq. (C.3).

JHEP01(2026)019

where $L_G^{\perp} = c\tau\gamma\beta\sin\theta$ with $\beta \equiv v/c$ and $\gamma \equiv 1/\sqrt{1-\beta^2} = (s - m_X + m_G^2)/(2m_G\sqrt{s})$ for $X = \gamma$, Z, and θ is the angle measured from the collider axis. With regard to the FCC-ee and CLIC, we assume the following data in our analysis: $R_{\rm FCC} = 0.5$ m , $\mathcal{L}_{\rm FCC_1} = 145\,{\rm ab}^{-1}$ for $\sqrt{s} = 91\,{\rm GeV}$, $\mathcal{L}_{\rm FCC_2} = 20\,{\rm ab}^{-1}$ for $\sqrt{s} = 161\,{\rm GeV}$, $\mathcal{L}_{\rm FCC_3} = 5{\rm ab}^{-1}$ for $\sqrt{s} = 250\,{\rm GeV}$ [25], and $R_{\rm CLIC} = 0.6$ m, $\mathcal{L}_{\rm CLIC} = 3\,{\rm ab}^{-1}$ for $\sqrt{s} = 3000\,{\rm GeV}$ [26].

To determine prospects of searches at lepton colliders, we largely followed the approach presented in ref. [36], which assumed zero background for the $e^+e^- \to {\rm ALP} + \gamma \to 3\gamma$ search, which is consistent with the results of [37] that determined the LEP [38] limits for photon-coupled ALP. While a sizable SM background from light hadrons and Z boson decays into two photons is expected [39], such events will be associated with the known mass and width of the decaying SM particle. Therefore, they can be vetoed, and their masses will be excluded from the projections for any BSM species also decaying into two photons. In fact, the recent reanalysis of the FCC sensitivity to the photon-coupled ALP [40] validated the results of [36] obtained under zero-background assumption, which also justifies our approach.

3.2 Long-lived regime

In fact, the KK gravitons decay predominantly into visible SM states, except the $\lambda^2 \gtrsim 1$ models in the region of the parameter space with light, $m_G \lesssim 10\,{\rm MeV}$, KK gravitons that decay mostly into other gravitons. In that case, however, the terrestrial experiments are typically not competitive with astrophysical bounds, as discussed in section 4. Therefore, beam dump experiments are more suitable to probe the long-lived regime of $\lambda^2 \lesssim 1$ GLD, in particular the RS and LD backgrounds, since there the KK gravitons decay predominantly into visible SM states.

Beam dump experiments. Beam dump experiments use a high-energy, $\sim 100\,{\rm GeV}$, electron/proton beam hitting a dense target, producing LLPs in the forward direction. The decay vessel, where LLPs decay into a pair of photons or charged SM states, is situated at a distance $\sim 100\,m$ from the production point, allowing to study LLP signature with highly displaced vertex. The background-free environment of beam dump experiments is achieved through spatial separation, magnetic deflection of charged particles, and the deployment of hadronic absorbers to suppress unwanted background of SM particles. We investigate visible decays of KK gravitons at beam dump experiments or forward LHC detectors: DUNE [41], FASER2 [42], MATHUSLA [43], NA62 [44], SeaQuest [45], and SHiP [46]; for each of them, we model their characteristics as given in table 1 of [47]. Let us highlight that the key distinction among these proposals stems from two factors: the distance between the production point and decay vessel, and the beam energy, which determine the probable lifetime scale and LLP boost factor, respectively. The minimal distance from LLP production point to the decay vessel ranges from $L_{\rm min} = 5\,m$ for SeaQuest, through $L_{\rm min} = 50\,m$ for SHiP, to FASER2, for which $L_{\rm min} = 480\,m$, covering intermediate lifetime regime. Consequently, beam dump experiments can probe intermediate LLP decay timescales that bridge the gap between collider searches and astrophysical or cosmological constraints.

JHEP01(2026)019

The number of LLP decays occurring within the detector positioned between $[L_{\rm min}, L_{\rm max}]$ from the production point is

$$N = \sum_{E,\theta} N_{\rm LLP}(E,\theta) \times \left(e^{-L_{\rm min}/d(E)} - e^{-L_{\rm max}/d(E)} \right), \tag{3.6}$$

where $N_{\rm LLP}(E,\theta)$ is the LLP spectrum, and the second factor corresponds to the probability of decays taking place inside a detector, and $d(E) = c\tau\gamma\beta$ is the decay length. Given that beam dump experiments are able to perform the search for high-energy displaced decays with essentially no background, guaranteed by large separation between LLP production and decay point, use of magnetic field and hadronic absorbers, we plot exclusion bounds based on $N = 3$ events.

The LLP spectrum, which describes the energy and angular distribution, is determined by rare meson decays, gauge boson (photon) fusion or conversion due to scattering or interaction with electromagnetic field, and bremsstrahlung, while other contributions are subdominant. The main production mode of $\lesssim$ GeV KK graviton G_k at beam dumps is Primakoff conversion, whose cross section is $\sigma_{\gamma N \to G_k N} \sim \alpha_{\rm EM} Z^2/(2\Lambda_k^2)$, where Z is the nucleus atomic number, and Λ_k is the coupling to two photons [47]. Moreover, KK gravitons can be produced via $B \to K + G_k$ decays. This mode of G_k production was neglected in [24, 48] because the energy momentum tensor involving (B, K) states is diagonal at leading order, and as a result this decay channel is loop-suppressed. In fact, explicit computation of such transition was done in [49], and we checked that it is indeed subdominant with respect to the Primakoff conversion.

FCC LLP mode. In e^+e^- collisions at high energies, in particular in the LLP mode of FCC-ee [50, 51], it is also possible to produce KK gravitons G_n from the decays of on-shell Z bosons, $Z \to G f\bar{f}$, where $f\bar{f}$ denotes SM fermions (mostly $b\bar{b}$ quarks). Although, the production of KK gravitons from Z boson decays is phase-space suppressed due to the three-body final state, yet the vast number of Z bosons produced at FCC-ee offsets this suppression, rendering it a feasible search channel. The number of KK gravitons in this mode is given by equation $N_{G_n} = N_Z \times {\rm BR}(Z \to G_n f\bar{f})$, where $N_Z = 2.5 \times 10^{12}$, while the averaged amplitude squared for this process is given by eq. (C.2). After KK graviton production, they decay into two photons or charged leptons, which is not a background-free search. To obtain the FCC-LLP bound, we apply the cuts on the energy and angular distribution of the final SM states, following the discussion in [50–52].

We note that since the gauge bosons are localized on the same brane, the $Z - \gamma - G_n$ coupling vanishes at tree level. The same coupling is induced radiatively, at 1-loop it was computed in refs. [53, 54], and it is suppressed by $\alpha_{\rm EM}^2$. As a result, it does not lead to competitive bounds.

Astrophysical bounds. In addition to the terrestrial searches, the long-lived regime can be probed by Big-Bang nucleosynthesis (BBN) [55], neutron stars (NS) observations (gamma rays and excess heating) [15, 56], and SN1987 [15, 57, 58]. We follow discussion in [15, 30, 56], except for the NS bounds, where we believe these limits determined in [15, 56] are in fact weaker by a factor ~ 2 — see appendix B. This affects only the $\lambda \gtrsim 1$ GLD models, since only very long-lived KK gravitons can survive for timescales relevant to NS.

JHEP01(2026)019

In particular, we note that the limit from the NS excess heating, $M_5 > 1.6 \times 10^5$ TeV, [15] does not correspond to the stated limit on the excess luminosity $L < L_{\max} = 10^{-5}\, L_\odot$, but instead corresponds to $L_{\max} = 4 \times 10^{-8}\, L_\odot$. In our analysis, we assume that this discrepancy is just a typo in the equation for $L_{\max}$, and that the correct limit on M_5 corresponds to $L_{\max} = 10^{-5}\, L_\odot$, which is also consistent with [59]. This means that the limit on M_5 for the ADD scenario with $n = 1$ extra dimensions is weaker by factor ~ 10, see the fourth row and the second column in table 1.

4 Experimental and astrophysical limits

The GLD with $\lambda^2 > 0$ has an approximate dilatonic shift symmetry,[7] which is softly broken by terms dependent on the curvature k. Therefore, the regime of k small compared to M_5 is technically natural. Since it involves light, weakly coupled KK states, it is quite difficult to probe and gathered relatively little phenomenological attention, although see [24, 30, 61]. Since the phenomenology of RS and LD at the LHC has been extensively studied [6, 16, 17, 62], we focus on the small curvature regime for these backgrounds. Adapting the discussion of [6] to the RS, see also section 3.1, we update the LHC bounds on this scenario as well. On the other hand, since phenomenology of GLD with $\lambda^2 > 1$ has not been studied before, we provide its comprehensive analysis according to the discussion in section 3, taking benchmark points $\lambda^2 = 2, 3, 4, 6, 10,$ and 100.

In figure 3, we show the current bounds and projected sensitivity of upcoming experiments to the previously introduced benchmarks of the GLD. The top panels correspond to RS and LD, $\lambda^2 = 0, 1$, respectively, while results for GLD with $\lambda^2 > 1$ are shown in the bottom panels. In all panels the gray-shaded regions indicate the currently excluded parameter space or theoretically disallowed parameter space with $k > M_5$, while the projected sensitivities of future experiments and astrophysical constraints are represented by solid, dashed, or dotted lines.

Let us first discuss the cases of RS ($\lambda^2 = 0$) and LD ($\lambda^2 = 1$). In RS and LD, the scale of the parameter k approximately corresponds to the mass scale of the lightest KK modes, while the parameter M_5 determines the size of the couplings of the KK modes with a given k. In the parameter space shown in figure 3, the KK graviton couplings allow for sizable production of the lightest KK gravitons at the LHC and lepton colliders. We show contours of fixed lifetime (expressed in meters) of the first massive KK graviton, $c\tau_{G_1}$, ranging from millimeter to kilometer, denoting the approximate range that can be covered from collider searches to astrophysical searches. For FCC-ee and CLIC we present two projections: assuming that all visible decay products (mostly gluons and quarks) of G_n can be detected (dashed), and only considering decays into a pair of photons (solid line). For the latter case, we also show lines (dotted) corresponding to 10, 100, and 1000 events, in case the zero-background assumption is not satisfied.[8] The parameter space with $k \gtrsim 1\,\text{GeV}$, which

[7] For $\lambda^2 = 0$, the Randall-Sundrum background, the low k/M_5 ratio is not natural, since the dilaton is decoupled. However, RS with small curvature k can be considered as a deformation of the ADD that significantly opens up the allowed parameter space by modifying the KK spectrum, which also leads to interesting collider signatures [24, 60].

[8] See the discussion for **electron-positron colliders** in section 3.1, especially the last paragraph.

JHEP01(2026)019

is currently covered up to $M_5 \sim 10\,\text{TeV}$ by the LHC [6, 16, 17, 62],[9] will be probed up to $M_5 \sim 200\,(100)\,\text{TeV}$ by CLIC and FCC-ee searches for G decays into a pair of any visible SM states (photons or leptons). The presented limits correspond to combined searches using $e^+e^- \to G\gamma$, $e^+e^- \to GZ$, and resonant production for both experiments. Because of the larger center-of-mass energy of CLIC and larger detector, it covers larger values of k than FCC-ee, which in turn covers most of the short-lived regime. The long-lived regime is covered by the BBN, SN1987, FCC-ee LLP, and beam dump experiments or forward LHC detectors: DUNE, FASER2, MATHUSLA, NA62, SeaQuest, and SHiP. The strongest terrestrial present constraints come from NuCal [63] and E137 [64]. We obtained a similar but slightly weaker exclusion line derived for E137 than the limits found in [30], which we believe is due to the neglect of the invisible decays (overwhelmingly into a pair of neutrinos, which constitute roughly 40% of the total decay width when $m_G \lesssim 2m_e$) of KK gravitons in [30].

Next, let us discuss the cases of the GLD models with $\lambda^2 > 1$. In contrast to RS and LD, the GLD models with $\lambda^2 > 1$ are characterized by continuum of densely packed KK states and small KK-graviton couplings similarly to the ADD model, while the KK-graviton couplings are proportional to some power of the KK-graviton masses. This gives rise to an interestingly distinctive feature that these models predict both a sizable flux of long-lived, light ($m_G \lesssim 30\,\text{MeV}$) KK gravitons, which lead to strong astrophysical bounds coming from SN observations, and comparably strong flux of heavy, $m_G \sim 1\,\text{TeV}$, KK gravitons decaying into visible SM states or invisible lighter KK states, which can be searched for by colliders. In the bottom figures in figure 3, both long-lived and short-lived KK gravitons can be produced at each parameter point (M_5, k), in contrast to the RS and LD scenarios. For the GLD model with $\lambda^2 = 2$ as a benchmark as shown in the bottom left panel, the LHC has excluded the parameter space up to $M_5 = k \sim 5\,\text{TeV}$, in addition to the tail occurring from the scaling of the total production cross section of the KK gravitons $\sigma_{\text{tot}} \sim \sum_n C_n^2/M_5^2 \sim k(\sqrt{s}/k)^q/(qM_5^3)$ with $q = (\lambda^2+2)/(\lambda^2-1)$ for the center-of-mass energy $\sqrt{s}$ of the collider. Moreover, CLIC will improve upon the LHC bounds by probing the parameter space up to $M_5 = k \sim 20\,\text{TeV}$, while FCC, due to its smaller center-of-mass energy, cannot produce heavy on-shell KK gravitons, resulting in the improvement by about an order of magnitude upon the limit set by LEP. On the other hand, displaced vertex searches for $\sim$GeV KK gravitons at SHiP and FCC LLP mode turn out to set weaker limits than the astrophysical bounds derived from SN1987 and other SN, which are sensitive to KK gravitons with masses $\lesssim 30\,\text{MeV}$. Finally, for $\lambda^2 \gtrsim 3$, the couplings of KK gravitons are too feeble to allow setting collider bound that would be competitive with the astrophysical limits. Therefore, in the bottom right panel of figure 3, we only show the relevant astrophysical bounds — the SN limits for $\lambda^2 = 3, 4$, and 6. The value $\lambda^2 = 6$ corresponds to the smallest parameter that can be realized in heterotic M-theory [13], and the resulting SN limits (denoted as SN1987 and Diffuse SNe at EGRET) approach to the $N = 1$ ADD limits as $k \to 0$, $M_5 \gtrsim 740\,\text{TeV}$ and $M_5 \gtrsim 3400\,\text{TeV}$, respectively — see table 1.

For the GLD models with $\lambda^2 \gtrsim 2$, we find that the decays of KK gravitons into lighter KK gravitons can become significant. We estimate the corresponding decay widths, using the

[9] The LHC LLP line denote the displaced vertex searches at the LHC, which, however, are not competitive with prompt searches due to short-lived nature of the gravitons produced in gluon/quark fusion.

JHEP01(2026)019

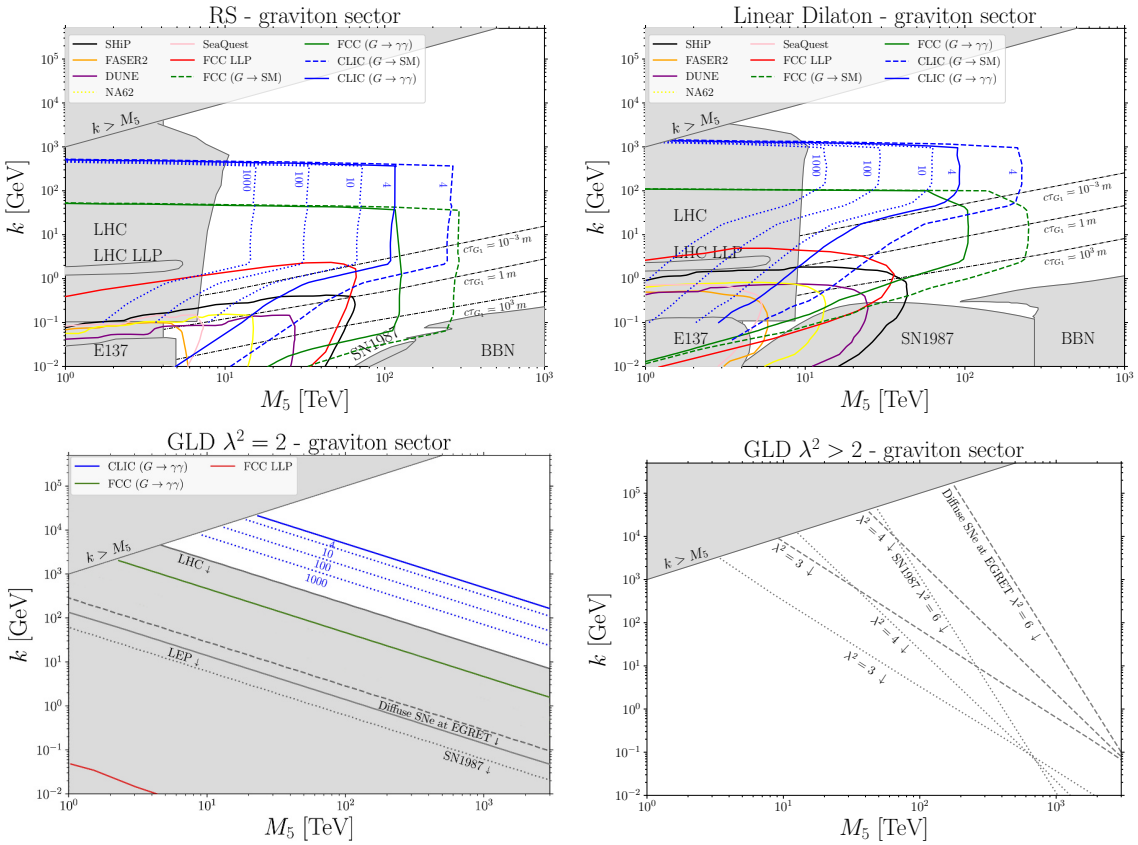

Figure 3. Limits and projections for the extra dimensional models obtained within the GLD. The results shown correspond to: the Randall-Sundrum model (*top left*), linear dilaton background (*top right*), generalized linear dilaton background with $\lambda^2 > 1$ (*bottom*). The RS and LD background correspond to $\lambda^2 = 0, 1$, respectively. The solid colorful lines indicate projections for future experiments, while grayed out regions are already excluded. The blue numbers $4, 10, 100, 1000$ denote the number of events at CLIC. The final sensitivity projection for CLIC and FCC corresponds to blue and green solid lines, respectively. The *bottom left* plot contains collider and astrophysical exclusion bounds — SN1987 (dotted) and Diffuse SNe at EGRET (dashed) — for $\lambda^2 = 2$, according to the legend. We also show astrophysical bounds on larger values of $\lambda^2 = 3, 4, 6$ (*bottom right*).

results of ref. [65], in particular eq. (A.6) therein.[10] For simplicity, let us consider decays into two identical light KK gravitons $G_n \to G_\ell G_\ell$ with $m_n \gg m_\ell$ for which the partial decay width is approximately estimated as

$$\Gamma_{G_n \to G_\ell G_\ell} \simeq \Gamma_{G_n \to \gamma\gamma} \times 2 \cdot 10^{-3} \times \left(\frac{m_n}{m_\ell}\right)^8 \times |\psi_{n\ell\ell}|^2 , \tag{4.1}$$

[10] Ref. [6] particularly studied the LD case ($\lambda^2 = 1$) and claimed that the $G_n \to \sum_{k,l} G_k G_l$ decays dominate over the decays into SM states if $k \ll M_5$ — see figure 26 and appendix D therein. We find that such inner KK tower decays are in fact negligible if $\lambda^2 \lesssim 2$ including the LD case ($\lambda^2 = 1$) if we use the three-graviton vertex formula of ref. [65] instead. According to [65], this difference is traced to the difference in the relative sign between the 4D Ricci scalar and 5D derivative contribution to the three-graviton vertex. Ref. [65] justified their formula by the fact that the unitarization of the graviton production amplitude does not go through with the other sign. Their formula was also confirmed by, e.g., ref. [66].

JHEP01(2026)019

where $\psi_{n\ell\ell}$ is the triple wavefunction overlap coefficient defined as

$$\psi_{nmk} = 2\, M_5^4 \int_0^{\pi R} dy\, e^{2ky}\, h_n(y)\, h_m(y)\, h_k(y) \tag{4.2}$$

with the graviton wavefunction $h_i(y)$ in eq. (2.21). We find it difficult to find an approximate analytic expression for the triple wavefunction overlap in GLD models with $\lambda^2 > 1$ which involves integration of three Bessel functions. Thus we numerically compute the triple wavefunction overlap and find that there exists a critical value of λ^2 above which the inner KK tower decays are dominant over other decays to SM particles. The critical value is around $\lambda^2 \simeq 2.4$. In contrast, below the critical value $\lambda^2 \lesssim 2.4$, the inner KK tower decays are negligible, unless the ratio k/M_5 is strongly suppressed, for example, $k/M_5 \lesssim 10^{-6}$ for $\lambda^2 = 2$. The existence of such a critical value of λ^2 can be understood by the fact that the factor $(m_n/m_\ell)^8 \propto \exp(8|p|\pi R) \sim (M_P\sqrt{k}/M_5^{3/2})^{16(\lambda^2-1)/(\lambda^2+2)}$ rapidly grows in λ^2.

Since astrophysical bounds strongly depend on the lifetimes of light KK gravitons, the inner KK tower decays are especially important when the mass gap is small, since then the KK gravitons with masses up to $\sim 10\,\text{MeV}$ have many possibilities of decays within the KK tower, potentially reducing their lifetimes. The strongest astrophysical bounds can come from observations of neutron stars (NS), which assume that LLPs have lifetimes at least as large as the corresponding neutron star. For flat extra dimensions, the KK tower decays are forbidden, and the KK gravitons have only feeble interactions with the SM, thus they are extremely long-lived. This regime is recovered for $\lambda^2 \gg 1$ when $k \ll M_5$, where we recover the following ADD limits [15, 56], see also appendix B: $M_5 > 740\,\text{TeV}$, $M_5 > 3400\,\text{TeV}$, and $M_5 > 1.2 \times 10^4\,\text{TeV}$, obtained by SN1987, Diffuse SNe at EGRET, and NS excess heating, respectively. On the other hand, in GLD with non-zero curvature, KK gravitons can have quite sizable interactions with other KK states, leading to much suppressed lifetimes, which relax the NS bounds. We show our results in figure 4 for $\lambda^2 = 6, 10, 100$, where one can see that taking into account the invisible decays (the left panel) leads to weaker bounds. Nonetheless, the SN1987 and EGRET SN limits — which are the same on both panels — are sufficiently strong to exclude GLD with $\lambda^2 \gg 1$ as a natural solution to the hierarchy problem.

5 Conclusions

In this work, we have examined the phenomenology of power-law warped extra dimensions realized by General Linear Dilaton models as well as updating the phenomenological prospects of the two conventional models, Randall-Sundrum and Linear Dilaton model. We updated or determined the current bounds on these models using the LHC searches, beam dumps, and astrophysical observations. Furthermore, we determined the sensitivity of future lepton colliders FCC-ee and CLIC, which will probe the $c\tau \lesssim 1\,m$ part of the parameter space for these models. As a result, the projected sensitivities extend the coverage up to $M_5 \sim 200\,\text{TeV}$, improving the current bounds by a factor ~ 20.

We also studied the long-lived regime, $c\tau \gg 1\,m$, particularly the region where the curvature scale k is small compared to the 5D Planck mass M_5. The low curvature regime is motivated due to an approximate shift symmetry of the dilaton. This regime can also

JHEP01(2026)019

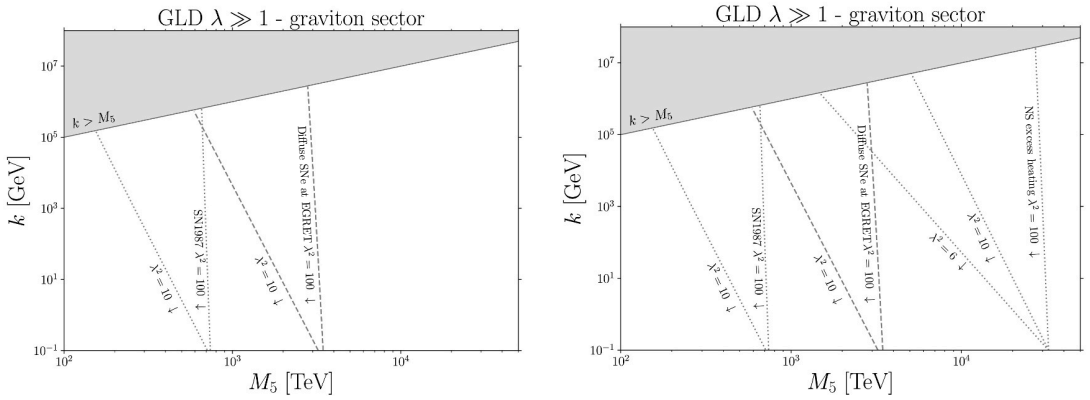

Figure 4. Limits on GLD with $\lambda^2 \gg 1$ with (left) and without (right) taking into account the KK tower decays of KK gravitons, which significantly shorten their lifetimes. As a result, light KK gravitons, which are produced in supernovae, decay before the neutron stars are formed and the corresponding bounds are evaded, as seen from the comparison of the left and right panels. On the other hand, the SN bounds are not affected, since the light KK gravitons are effectively stable on this timescale.

be interpreted as deformations of the flat ADD scenario with only one additional space dimension, which avoids stringent bounds due to warping.

We determined the prospects of the currently running or approved beam dump experiments like FASER, NA62, and SHiP, and the proposed DUNE, MATHUSLA, and SeaQuest, for detecting decays of ∼sub-GeV KK gravitons. We also demonstrated their synergy with the searches at the LLP mode of FCC-ee utilizing the Z boson decays. Consequently, future experiments will therefore comprehensively test both the short and long-lived parameter space of the GLD models.

Generalizing the observations made in [6] for the LD, GLD with $\lambda^2 > 1$ leads to a different phenomenology from both ADD and RS models due to its different structure of KK states — their masses and couplings. In particular, KK gravitons are characterized by a compressed spectrum leading to cascade decays into high-energy SM particles. If such a signal emerges in searches for long-lived particles, it could be a smoking gun signature of a power-law warped extra dimension. Moreover, we studied the corresponding astrophysical bounds, where we found that the observations of SN1987 and neutron stars can place the most stringent bounds for GLD with $\lambda^2 \gtrsim 1$. In particular, our revised astrophysical bounds on ADD scenario with 1 extra dimension (corresponding to $\lambda^2 \to \infty$), are weaker than stated in the literature [15, 56] by a factor ~ 2. Our results may therefore motivate further phenomenological and experimental efforts to investigate the GLD.

Acknowledgments

KJ thanks Stephen Angus, Brian Batell, Sungwoo Hong, Fotis Koutroulis, Miguel Montero, Georg Raffelt, and Seokhoon Yun for useful discussions or remarks. We also thank Steen Hannestad and Georg Raffelt for correspondence and for updating ref. [15]. This work was supported by IBS under the project code, IBS-R018-D1.

JHEP01(2026)019

Note added. In the first version of this paper, which appeared on the arXiv on Dec. 31, 2024, we pointed out *two* numerical inconsistencies in previous works devoted to astrophysical bounds on the ADD model with n extra dimensions [15, 56], which set the most stringent limits for $n < 4$. We provided corrected limits on ADD, by following the methodology of [15] but using the correct numerical values for the decay widths of KK gravitons and the constraint on neutron stars excess heating, $L_{\rm max} \lesssim L_\odot \times 10^{-5}$. This was confirmed in the recently updated (March 31, 2025) version of ref. [15], whose final results are consistent with our analysis. Therefore, we expect our results shown in figure 3 and 4 to be robust. In particular, for our case, where $n = 1$ ADD limit is relevant, the strongest limit turns out to come from analysis of the whole population of neutron stars located in the central bulge of the Milky Way [56]. Their analysis has also been affected by numerical error, and the updated bound for $n = 1$ reads $M_5 > 3.6 \times 10^4$ TeV — see table 1.

A Background solution for the GLD model

The GLD action in the Einstein frame is given in eq. (2.3):

$$\mathcal{S} = \int d^4x \int_{-\pi R}^{\pi R} dy \sqrt{-g} M_5^3 \left(\frac{1}{2}\mathcal{R} - \frac{1}{2}\partial^M S \partial_M S - V(S) - V^b(S) \right), \tag{A.1}$$

where

$$V(S) = -2k_b^2 e^{-2\lambda S/\sqrt{3}}, \tag{A.2}$$

$$V^b(S) = -\frac{e^{-\lambda S/\sqrt{3}}}{\sqrt{g_{55}}} \left[4k_0 \delta(y) + 4k_\pi \delta(y - \pi R) \right]. \tag{A.3}$$

Let us take an ansatz for the metric as

$$ds^2 = e^{2\sigma_1(y)} \eta_{\mu\nu} dx^\mu dx^\nu + e^{2\sigma_2(y)} dy^2. \tag{A.4}$$

This metric has to satisfy the Einstein equation. The Einstein equation is

$$G_{MN} = \frac{1}{M_5^3} T_{MN}, \tag{A.5}$$

where

$$G_{MN} = \mathcal{R}_{MN} - \frac{1}{2} g_{MN} \mathcal{R}, \tag{A.6}$$

$$\frac{1}{M_5^3} T_{MN} = \partial_M S \partial_N S - g_{MN} \left(\frac{1}{2} g^{AB} \partial_A S \partial_B S + V(S) + V^b(S) \right) + \delta_{M5} \delta_{N5}\, g_{MN} V^b(S). \tag{A.7}$$

The $\mu\nu$-components of the Einstein equation gives

$$\begin{aligned} &3\left(\sigma_1'' + 2(\sigma_1')^2 - \sigma_1'\sigma_2'\right) = \\ &\qquad -\frac{1}{2}(S')^2 + 2k_b^2 e^{2(\sigma_2 - \lambda S/\sqrt{3})} - e^{\sigma_2 - \lambda S/\sqrt{3}} \left[-4k_0 \delta(y) - 4k_\pi \delta(y - \pi R) \right], \end{aligned} \tag{A.8}$$

JHEP01(2026)019

while the 55-component yields

$$6(\sigma_1')^2 = \frac{1}{2}(S')^2 + 2k_b^2 e^{2(\sigma_2 - \lambda S/\sqrt{3})}. \tag{A.9}$$

Here the prime ($'$) denotes the derivative with respect to the coordinate y. Combining eq. (A.8) and eq. (A.9), we obtain

$$3\sigma_1'' - 3\sigma_1'\sigma_2' + S'^2 = -e^{\sigma_2 - \lambda S/\sqrt{3}}\left[-4k_0\delta(y) - 4k_\pi\delta(y-\pi R)\right], \tag{A.10}$$

$$12\sigma_1'^2 - S'^2 = 4k_b^2 e^{2(\sigma_2 - \lambda S/\sqrt{3})}. \tag{A.11}$$

On the other hand, the equation of motion for S is

$$\partial_M(\sqrt{-g}g^{MN}\partial_N S) = \sqrt{-g}\frac{\partial}{\partial S}(V(S) + V^b(S)), \tag{A.12}$$

which gives

$$\sqrt{3}S'' + \sqrt{3}(4\sigma_1' - \sigma_2')S' = 4\lambda k_b^2 e^{2(\sigma_2 - \lambda S/\sqrt{3})} - \lambda e^{\sigma_2 - \lambda S/\sqrt{3}}\left[-4k_0\delta(y) - 4k_\pi\delta(y-\pi R)\right]. \tag{A.13}$$

We find a solution to the equations of motion in eq. (A.10), eq. (A.11), and eq. (A.13) as

$$\sigma_1 = k_1|y| + c_1, \tag{A.14}$$

$$\sigma_2 = k_2|y| + c_2, \tag{A.15}$$

$$\frac{\lambda}{\sqrt{3}}S = \sigma_2 + \frac{\lambda}{\sqrt{3}}S_0, \tag{A.16}$$

$$k_2 = \lambda^2 k_1 = \frac{2\lambda^2}{\sqrt{3(4-\lambda^2)}}k_b\, e^{-\lambda S_0/\sqrt{3}}, \tag{A.17}$$

$$k_0\, e^{-\lambda S_0/\sqrt{3}} = -k_\pi\, e^{-\lambda S_0/\sqrt{3}} = \frac{3}{2}k_1, \tag{A.18}$$

where c_1, c_2, and S_0 are some constants. The constants c_1 and c_2 can be absorbed by a coordinate transformation as follows without loss of generality.

$$x^\mu \to e^{-c_1}x^\mu, \quad y \to ye^{-c_2}. \tag{A.19}$$

On the other hand, the constant S_0 corresponds to the vacuum expectation value of S at $y = 0$, which may be determined by an additional brane potential [6]. S_0 determines physical curvature scale of the extra dimension by

$$\begin{aligned} k_b^{\rm phy} &= k_b e^{-\lambda S_0/\sqrt{3}}, \\ k_0^{\rm phy} &= k_0 e^{-\lambda S_0/\sqrt{3}}, \\ k_\pi^{\rm phy} &= k_\pi e^{-\lambda S_0/\sqrt{3}}. \end{aligned} \tag{A.20}$$

JHEP01(2026)019

B Astrophysical bounds on large extra dimensions

The Lagrangian describing KK gravitons interactions with the SM is given by eq. (2.29), which we write in the following form:

$$\mathcal{L} \supset -\frac{1}{\Lambda_n} h_{\mu\nu}^{(n)} T_{\rm SM}^{\mu\nu} \tag{B.1}$$

which allows to compute, e.g., the decay widths of KK gravitons. Since astrophysical bounds affect only light gravitons, the relevant decay channels are $\gamma\gamma$, $\nu\nu$, and e^+e^-. The analytical forms of the decay widths that were used in [15, 56] are given in [35]. The decay widths were also obtained in, e.g., ref. [67], which confirmed these results up to a factor of 1/4 for each decay width — the difference originates in the extra factor of 1/2 in the Lagrangian of [35] — compare eq. 33 in [35] to eq. 4 in [67] — we follow the convention of [67].

We note that there is an inconsistency in *numerical* values for lifetimes of gravitons given by eq. 47 and 50 in ref. [35]. Indeed, in the limit $m_G \gg m_V$, where V indicates a massive gauge boson,

$$\tau_{G\to VV} \simeq \frac{5\times 10^2}{\kappa^2 m_G^3} \simeq \frac{1}{2}\tau_{G\to\gamma\gamma} \simeq 30\,{\rm yr}\left(\frac{100\,{\rm GeV}}{m_G}\right)^3 = 3\times 10^{10}\,{\rm yr}\left(\frac{0.1\,{\rm GeV}}{m_G}\right)^3, \tag{B.2}$$

which is larger than the value given by eq. 47, $\tau_{G\to\gamma\gamma} \simeq 6\times 10^9\,{\rm yr}\left(\frac{0.1\,{\rm GeV}}{m_G}\right)^3$ by a factor of 10.

Let us briefly recall the results of ref. [15]. The rate at which a single graviton loses energy is determined by

$$Q_n = \frac{1}{\Lambda_n^2}\sigma_N n_B^2 T^{7/2} m_N^{-1/2}\,, \tag{B.3}$$

and to obtain the total rate, one needs to sum over all the $n \in \mathbb{N}$. Since the mass splitting between consecutive gravitons is small (with exception of the RS in the $k \simeq M_5$ region), and since we consider models with $n = 1$ extra dimensions, one can substitute the summation with the following integration measure:

$$\sum_n \to 2\int \left|\frac{dn}{dm}\right| dm\,, \tag{B.4}$$

where $\left|\frac{dn}{dm}\right| = 1/\left|\frac{dm}{dn}\right|$ can be easily computed from eq. (2.25).

In table 1, we present the results of our analysis. We stress that i) we followed the methodology developed in [15, 68, 69] to obtain the relevant fluxes, in particular eq. 28, 47, and 55 in [15] and ii) we did not attempt to update the limits by using more modern data. Regarding the first point, our improvements are due to *numerical* factors, while the relevant analytical expressions in the mentioned papers, e.g., [15, 35, 56] are unchanged. As for the latter point, we leave such task for a future work.

We believe that the difference between our limits and those given in [15, 56] stems from the fact that both of these papers used eq. 47 from [35], which is too small by a factor of 10.[11]

[11] Note that for light KK gravitons, the total decay width satisfies $\tau = 1/\Gamma = 1/(\Gamma_{\gamma\gamma} + \Gamma_{3\nu\nu} + \Gamma_{e^+e^-}) = 1/(2.25\Gamma_{\gamma\gamma})$, and the branching ratio into two photons is $\simeq 0.5$. However, eq. 44 in [15] directly follows eq. 47 from [35], and therefore the factor γ in eq. 46 in [15] is too large by a factor of 10; we believe that ref. [56] used the same formula — see the equation without number described in the sentence "and thus their lifetime..." and eq. 1 therein. Therefore, the photon flux given by eq. 47, 55 in [15] and eq. 1 in [56] was overestimated by 1 order of magnitude.

JHEP01(2026)019

n	1	2	3	4	5	6	7
SN 1987A (HR)	(7.4×10^2)	(8.9)	(0.66)	(1.18×10^{-1})	(3.5×10^{-2})	(1.44×10^{-2})	(7.2×10^{-3})
EGRET SNe (HR)	(3.4×10^3)	(28)	(1.65)	(2.54×10^{-1})	(6.8×10^{-2})	(2.56×10^{-2})	(1.21×10^{-2})
NS excess heat (HR)	1.2×10^4 (1.61×10^5)	100 (7.01×10^2)	5.3 (25.5)	0.75 (2.77)	0.2 (0.57)	0.065 (0.17)	2.84×10^{-2} (6.84×10^{-2})
EGRET NS (HR)	1.4×10^3 (2.93×10^3)	22 (38.6)	1.7 (2.65)	0.3 (0.43)	0.084 (0.116)	3.3×10^{-2} (4.31×10^{-2})	1.53×10^{-2} (1.98×10^{-2})
EGRET NS - GB (CPBS)	3.6×10^4 (7.8×10^4)	2.5×10^2 (4.5×10^2)	12 (19)	1.5 (2.2)	3.4×10^{-1} (4.7×10^{-1})	1.1×10^{-1} (1.47×10^{-1})	4.6×10^{-2} (5.9×10^{-2})

Table 1. Our limits on ADD parameter $\bar{M}_{4+n}$ [TeV] obtained by following the discussion in [15]. In parentheses, we indicate limits obtained by HR [15] and CPBS [56].

n	1	2	3	4	5	6	7
SN 1987A (HR)	(4.9×10^2)	(9.6×10^{-7})	(1.14×10^{-9})	(3.82×10^{-11})	(4.85×10^{-12})	(1.21×10^{-12})	(4.42×10^{-13})
EGRET SNe (HR)	(4.9)	(9.6×10^{-8})	(2.47×10^{-10})	(1.21×10^{-11})	(1.93×10^{-12})	(5.6×10^{-13})	(2.29×10^{-13})
NS excess heat (HR)	1.22×10^{-1} (4.44×10^{-5})	8.16×10^{-9} (1.55×10^{-10})	3.6×10^{-11} (2.58×10^{-12})	2.43×10^{-12} (3.36×10^{-13})	4.85×10^{-13} (9.95×10^{-14})	1.65×10^{-13} (4.41×10^{-14})	7.63×10^{-14} (2.46×10^{-14})
EGRET NS (HR)	73.6 (7.36)	1.6×10^{-7} (5.13×10^{-8})	2.4×10^{-10} (1.12×10^{-10})	9.8×10^{-12} (5.46×10^{-12})	1.46×10^{-12} (9.13×10^{-13})	4.1×10^{-13} (2.8×10^{-13})	1.7×10^{-13} (1.21×10^{-13})
EGRET NS - GB (CPBS)	3.9×10^{-3} (3.9×10^{-4})	1.2×10^{-9} (3.8×10^{-10})	9.1×10^{-12} (4.2×10^{-12})	8.3×10^{-13} (4.7×10^{-13})	2×10^{-13} (1.3×10^{-13})	8×10^{-14} (5.4×10^{-14})	4.1×10^{-14} (2.9×10^{-14})

Table 2. Same as table 1 but the limits are given on the parameter R $[m]$.

Moreover, the NS excess heat bound on $\bar{M}_{4+n}$ stated in table VI of ref. [15], corresponds to $L_{\rm max} \lesssim L_\odot \times 5 \times 10^{-8}$, instead of the stated limit $L_{\rm max} \leq L_\odot \times 10^{-5}$ (factor of ~ 200 difference). We were unable to trace the source of this discrepancy; we assume that the limit on $L_{\rm max}$ is $L_\odot \times 10^{-5}$, as written in ref. [15],[12] the paragraph below eq. 56, since this is the result of [59]. Therefore, the effective photon flux relevant to the NS excess heat bound on $\bar{M}_{4+n}$ is weakened by a total factor of $\sim 10 \times 200 = 2000$ with respect to ref. [15]. For an easy comparison with the tables from [15], in table 2, we give both the upper limits on R [m] and the lower limits on $\overline{M}_{4+n}$ [TeV]. Note that in the main body of our work, we consider $n = 1$, i.e., $M_5 = \overline{M}_5$ in the notation of [15]; GB stands for Galactic bulge, and, for completeness, we also show the SNe limits from ref. [15], which are unaffected.

[12]We also thank Georg Raffelt for correspondence on this point.

JHEP01(2026)019

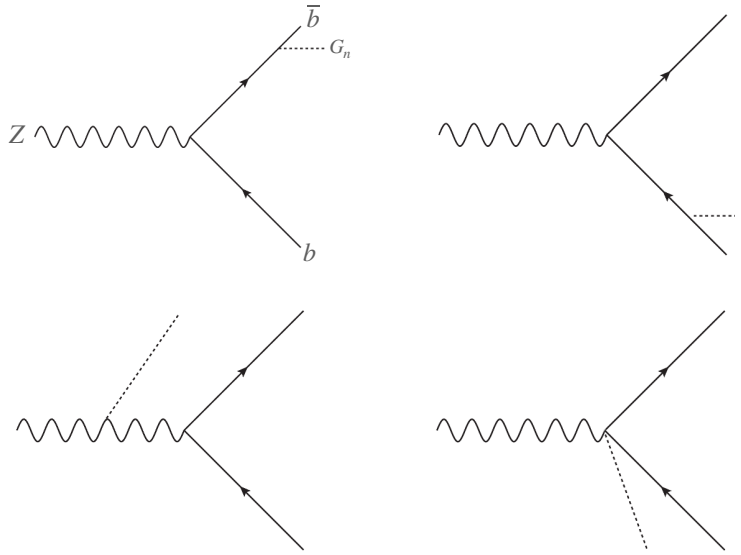

Figure 5. Feynman diagrams contributing to $Z \to f\bar{f}G_n$. The $e^+e^- \to G_nZ$ process is described by the same diagrams by using the crossing symmetry relations between the Mandelstam variables.

C Cross sections

Below we provide the averaged amplitudes squared for the processes relevant to our analyses: $e^+e^- \to G_n\gamma$ or $e^+e^- \to G_nZ$ at FCC-ee and CLIC, and $Z \to f\bar{f}G_n$, where f is charged SM fermion, at LLP mode of FCC-ee. The Feynman diagrams describing the latter process are shown in figure 5. In order to obtain the corresponding cross sections, we follow the discussion in the kinematics section of the Particle Data Group [70]. In particular, s and t denote the Mandelstam variables.

$$
\begin{aligned}
|M|^2_{e^+e^-\to G_nZ} = &-\frac{e^2\left(g_A^2+g_V^2\right)}{12\Lambda^2t^2\left(\Gamma_Z^2m_Z^2+\left(m_Z^2-s\right)^2\right)\left(m_{G_n}^2+m_Z^2-s-t\right)^2}\times \\
&\Big[3m_{G_n}^8\left(m_Z^6-m_Z^4(2s+t)+m_Z^2s(s+2t)-st(s+4t)\right) \\
&+m_{G_n}^6\Big(6m_Z^8-3m_Z^6(6s+5t)+m_Z^4\left(18s^2+57st+13t^2\right) \\
&-m_Z^2\left(6s^3+45s^2t+90st^2+4t^3\right)+3st\left(s^2+11st+16t^2\right)\Big) \\
&+m_{G_n}^4\Big(3m_Z^{10}-3m_Z^8(4s+5t)+2m_Z^6\left(9s^2+45st+16t^2\right) \\
&-2m_Z^4\left(6s^3+57s^2t+110st^2+16t^3\right)+3m_Z^2\left(s^4+14s^3t+64s^2t^2+76st^3+4t^4\right) \\
&-3st\left(s^3+12s^2t+36st^2+28t^3\right)\Big) \\
&+m_{G_n}^2t\Big(-3m_Z^{10}+m_Z^8(33s+13t)-2m_Z^6\left(30s^2+75st+16t^2\right) \\
&+m_Z^4\left(36s^3+206s^2t+276st^2+34t^3\right)-3m_Z^2\left(3s^4+34s^3t+96s^2t^2+76st^3+4t^4\right)
\end{aligned}
\tag{C.1}
$$

JHEP01(2026)019

$$
\begin{aligned}
&+3s\left(s^4+11s^3t+36s^2t^2+50st^3+24t^4\right)\Big)-4t^2\left(-m_Z^2+s+t\right)^2\times\\
&\left(m_Z^4(5s+t)-m_Z^2t(7s+t)+3s\left(s^2+2st+2t^2\right)\right)\Big],
\end{aligned}
$$

$$
\begin{aligned}
|M|^2_{Z\to G_n e^+e^-} = &-\frac{e^2\left(g_A^2+g_V^2\right)}{12\Lambda^2 s_{12}^2\left(\Gamma_Z^2m_Z^2+\left(m_Z^2-s_{23}\right)^2\right)\left(m_{G_n}^2+m_Z^2-s_{12}-s_{23}\right)^2}\times \\
&\Big[3m_{G_n}^8\left(m_Z^6-m_Z^4(s_{12}+2s_{23})+m_Z^2s_{23}(2s_{12}+s_{23})-s_{12}s_{23}(4s_{12}+s_{23})\right)\\
&+m_{G_n}^6\Big(6m_Z^8-3m_Z^6(5s_{12}+6s_{23})+m_Z^4\left(13s_{12}^2+57s_{12}s_{23}+18s_{23}^2\right)\\
&-m_Z^2\left(4s_{12}^3+90s_{12}^2s_{23}+45s_{12}s_{23}^2+6s_{23}^3\right)+3s_{12}s_{23}\left(16s_{12}^2+11s_{12}s_{23}+s_{23}^2\right)\Big)\\
&+m_{G_n}^4\Big(3m_Z^{10}-3m_Z^8(5s_{12}+4s_{23})+2m_Z^6\left(16s_{12}^2+45s_{12}s_{23}+9s_{23}^2\right)\\
&-2m_Z^4\left(16s_{12}^3+110s_{12}^2s_{23}+57s_{12}s_{23}^2+6s_{23}^3\right)\\
&+3m_Z^2\left(4s_{12}^4+76s_{12}^3s_{23}+64s_{12}^2s_{23}^2+14s_{12}s_{23}^3+s_{23}^4\right)\\
&-3s_{12}s_{23}\left(28s_{12}^3+36s_{12}^2s_{23}+12s_{12}s_{23}^2+s_{23}^3\right)\Big)\\
&+m_{G_n}^2s_{12}\Big(-3m_Z^{10}+m_Z^8(13s_{12}+33s_{23})-2m_Z^6\left(16s_{12}^2+75s_{12}s_{23}+30s_{23}^2\right)\\
&+m_Z^4\left(34s_{12}^3+276s_{12}^2s_{23}+206s_{12}s_{23}^2+36s_{23}^3\right)\\
&-3m_Z^2(4s_{12}^4+76s_{12}^3s_{23}+96s_{12}^2s_{23}^2+34s_{12}s_{23}^3+3s_{23}^4)\\
&+3s_{23}\left(24s_{12}^4+50s_{12}^3s_{23}+36s_{12}^2s_{23}^2+11s_{12}s_{23}^3+s_{23}^4\right)\Big)\\
&-4s_{12}^2\left(-m_Z^2+s_{12}+s_{23}\right)^2\times\\
&\times\left(m_Z^4(s_{12}+5s_{23})-m_Z^2s_{12}(s_{12}+7s_{23})+3s_{23}\left(2s_{12}^2+2s_{12}s_{23}+s_{23}^2\right)\right)\Big],
\end{aligned}
\tag{C.2}
$$

$$
|M|^2_{e^+e^-\to G_n}\simeq\frac{\pi s^2}{10\Lambda^2}, \tag{C.3}
$$

where G_n is a KK graviton with mass m_{G_n} and universal coupling Λ, we neglected the masses of the electrons, and $g_V = 1/(4\sin\theta_W\cos\theta_W)$, $g_A = 1/(4\sin\theta_W\cos\theta_W)(1-4\sin^2\theta_W)$. Analogous formula holds for the Z decays involving quarks, e.g., $Z\to G_nb\bar{b}$, where one replaces the fermion masses and couplings in trivial way. The ranges of the integration variables, s_{23} and s_{12}, are taken from the PDG.

Data Availability Statement. This article has no associated data or the data will not be deposited.

Code Availability Statement. This article has no associated code or the code will not be deposited.

JHEP01(2026)019

References

[1] J. Polchinski, *String theory. Vol. 1: An introduction to the bosonic string*, Cambridge University Press (2007) [DOI:10.1017/CBO9780511816079] [INSPIRE].

[2] D. Tong, *String Theory*, arXiv:0908.0333 [INSPIRE].

[3] N. Arkani-Hamed, S. Dimopoulos and G.R. Dvali, *The hierarchy problem and new dimensions at a millimeter*, *Phys. Lett. B* **429** (1998) 263 [hep-ph/9803315] [INSPIRE].

[4] L. Randall and R. Sundrum, *A large mass hierarchy from a small extra dimension*, *Phys. Rev. Lett.* **83** (1999) 3370 [hep-ph/9905221] [INSPIRE].

[5] I. Antoniadis, A. Arvanitaki, S. Dimopoulos and A. Giveon, *Phenomenology of TeV Little String Theory from Holography*, *Phys. Rev. Lett.* **108** (2012) 081602 [arXiv:1102.4043] [INSPIRE].

[6] G.F. Giudice et al., *Clockwork/linear dilaton: structure and phenomenology*, *JHEP* **06** (2018) 009 [arXiv:1711.08437] [INSPIRE].

[7] G.F. Giudice and M. McCullough, *A Clockwork Theory*, *JHEP* **02** (2017) 036 [arXiv:1610.07962] [INSPIRE].

[8] K. Choi, H. Kim and S. Yun, *Natural inflation with multiple sub-Planckian axions*, *Phys. Rev. D* **90** (2014) 023545 [arXiv:1404.6209] [INSPIRE].

[9] K. Choi and S.H. Im, *Realizing the relaxion from multiple axions and its UV completion with high scale supersymmetry*, *JHEP* **01** (2016) 149 [arXiv:1511.00132] [INSPIRE].

[10] D.E. Kaplan and R. Rattazzi, *Large field excursions and approximate discrete symmetries from a clockwork axion*, *Phys. Rev. D* **93** (2016) 085007 [arXiv:1511.01827] [INSPIRE].

[11] K. Choi, S.H. Im and C.S. Shin, *General Continuum Clockwork*, *JHEP* **07** (2018) 113 [arXiv:1711.06228] [INSPIRE].

[12] A. Lukas, B.A. Ovrut, K.S. Stelle and D. Waldram, *Heterotic M theory in five-dimensions*, *Nucl. Phys. B* **552** (1999) 246 [hep-th/9806051] [INSPIRE].

[13] S.H. Im, H.P. Nilles and M. Olechowski, *Heterotic M-Theory from the Clockwork Perspective*, *JHEP* **01** (2019) 151 [arXiv:1811.11838] [INSPIRE].

[14] D. Teresi, *Clockwork without supersymmetry*, *Phys. Lett. B* **783** (2018) 1 [arXiv:1802.01591] [INSPIRE].

[15] S. Hannestad and G.G. Raffelt, *Supernova and neutron star limits on large extra dimensions reexamined*, *Phys. Rev. D* **67** (2003) 125008 [*Erratum ibid.* **69** (2004) 029901] [hep-ph/0304029] [INSPIRE].

[16] ATLAS collaboration, *Search for new high-mass phenomena in the dilepton final state using 36 fb^{-1} of proton-proton collision data at $\sqrt{s} = 13$ TeV with the ATLAS detector*, *JHEP* **10** (2017) 182 [arXiv:1707.02424] [INSPIRE].

[17] CMS collaboration, *Search for new resonances in the diphoton final state in the mass range between 70 and 110 GeV in pp collisions at $\sqrt{s} = 8$ and 13 TeV*, CMS-PAS-HIG-17-013 (2017) [INSPIRE].

JHEP01(2026)019

[18] G. Lanfranchi, M. Pospelov and P. Schuster, *The Search for Feebly Interacting Particles*, *Ann. Rev. Nucl. Part. Sci.* **71** (2021) 279 [arXiv:2011.02157] [INSPIRE].

[19] E. Witten, *Dimensional Reduction of Superstring Models*, *Phys. Lett. B* **155** (1985) 151 [INSPIRE].

[20] M. Dine and N. Seiberg, *Couplings and Scales in Superstring Models*, *Phys. Rev. Lett.* **55** (1985) 366 [INSPIRE].

[21] P. Artoisenet et al., *A framework for Higgs characterisation*, *JHEP* **11** (2013) 043 [arXiv:1306.6464] [INSPIRE].

[22] J.A. Gill, D. Sengupta and A.G. Williams, *Graviton-photon production with a massive spin-2 particle*, *Phys. Rev. D* **108** (2023) L051702 [arXiv:2303.04329] [INSPIRE].

[23] I. Antoniadis, S. Dimopoulos and A. Giveon, *Little string theory at a TeV*, *JHEP* **05** (2001) 055 [hep-th/0103033] [INSPIRE].

[24] G.F. Giudice, T. Plehn and A. Strumia, *Graviton collider effects in one and more large extra dimensions*, *Nucl. Phys. B* **706** (2005) 455 [hep-ph/0408320] [INSPIRE].

[25] FCC collaboration, *FCC-ee: The Lepton Collider: Future Circular Collider Conceptual Design Report Volume 2*, *Eur. Phys. J. ST* **228** (2019) 261 [INSPIRE].

[26] CLIC and CLICDP collaborations, *Updated baseline for a staged Compact Linear Collider*, *CERN Yellow Rep.* **4** (2016) 1 [arXiv:1608.07537] [INSPIRE].

[27] A.D. Martin, W.J. Stirling, R.S. Thorne and G. Watt, *Parton distributions for the LHC*, *Eur. Phys. J. C* **63** (2009) 189 [arXiv:0901.0002] [INSPIRE].

[28] D.B. Clark, E. Godat and F.I. Olness, *ManeParse : A Mathematica reader for Parton Distribution Functions*, *Comput. Phys. Commun.* **216** (2017) 126 [arXiv:1605.08012] [INSPIRE].

[29] A. Buckley et al., *LHAPDF6: parton density access in the LHC precision era*, *Eur. Phys. J. C* **75** (2015) 132 [arXiv:1412.7420] [INSPIRE].

[30] M. Baryakhtar, *Graviton Phenomenology of Linear Dilaton Geometries*, *Phys. Rev. D* **85** (2012) 125019 [arXiv:1202.6674] [INSPIRE].

[31] CMS collaboration, *Search for physics beyond the standard model in the high-mass diphoton spectrum at* 13 TeV, CMS-PAS-EXO-17-017 (2018) [INSPIRE].

[32] S. Knapen and S. Lowette, *A Guide to Hunting Long-Lived Particles at the LHC*, *Ann. Rev. Nucl. Part. Sci.* **73** (2023) 421 [arXiv:2212.03883] [INSPIRE].

[33] M. Drewes and J. Hajer, *Heavy Neutrinos in displaced vertex searches at the LHC and HL-LHC*, *JHEP* **02** (2020) 070 [arXiv:1903.06100] [INSPIRE].

[34] G.F. Giudice, R. Rattazzi and J.D. Wells, *Quantum gravity and extra dimensions at high-energy colliders*, *Nucl. Phys. B* **544** (1999) 3 [hep-ph/9811291] [INSPIRE].

[35] T. Han, J.D. Lykken and R.-J. Zhang, *On Kaluza-Klein states from large extra dimensions*, *Phys. Rev. D* **59** (1999) 105006 [hep-ph/9811350] [INSPIRE].

[36] M. Bauer, M. Heiles, M. Neubert and A. Thamm, *Axion-Like Particles at Future Colliders*, *Eur. Phys. J. C* **79** (2019) 74 [arXiv:1808.10323] [INSPIRE].

[37] S. Knapen, T. Lin, H.K. Lou and T. Melia, *Searching for Axionlike Particles with Ultraperipheral Heavy-Ion Collisions*, *Phys. Rev. Lett.* **118** (2017) 171801 [arXiv:1607.06083] [INSPIRE].

[38] OPAL collaboration, *Multiphoton production in e^+e^- collisions at $\sqrt{s} = 181$ GeV to 209 GeV*, *Eur. Phys. J. C* **26** (2003) 331 [hep-ex/0210016] [INSPIRE].

JHEP01(2026)019

[39] D. d'Enterria and V.D. Le, *Rare and exclusive few-body decays of the Higgs, Z, W bosons, and the top quark*, *J. Phys. G* **52** (2025) 053001 [arXiv:2312.11211] [INSPIRE].

[40] P. Rebello Teles, D. d'Enterria, V.P. Gonçalves and D.E. Martins, *Searches for axionlike particles via $\gamma\gamma$ fusion at future e^+e^- colliders*, *Phys. Rev. D* **109** (2024) 055003 [arXiv:2310.17270] [INSPIRE].

[41] DUNE collaboration, *Deep Underground Neutrino Experiment (DUNE), Far Detector Technical Design Report, Volume II: DUNE Physics*, arXiv:2002.03005 [INSPIRE].

[42] FASER collaboration, *FASER's physics reach for long-lived particles*, *Phys. Rev. D* **99** (2019) 095011 [arXiv:1811.12522] [INSPIRE].

[43] D. Curtin et al., *Long-Lived Particles at the Energy Frontier: The MATHUSLA Physics Case*, *Rept. Prog. Phys.* **82** (2019) 116201 [arXiv:1806.07396] [INSPIRE].

[44] NA62 collaboration, *Dark Sectors at fixed targets: The example of NA62*, *Frascati Phys. Ser.* **66** (2018) 312 [arXiv:1807.10170] [INSPIRE].

[45] A. Berlin, S. Gori, P. Schuster and N. Toro, *Dark Sectors at the Fermilab SeaQuest Experiment*, *Phys. Rev. D* **98** (2018) 035011 [arXiv:1804.00661] [INSPIRE].

[46] S. Alekhin et al., *A facility to Search for Hidden Particles at the CERN SPS: the SHiP physics case*, *Rept. Prog. Phys.* **79** (2016) 124201 [arXiv:1504.04855] [INSPIRE].

[47] K. Jodłowski, *Probing some photon portals to new physics at intensity frontier experiments*, *Phys. Rev. D* **108** (2023) 115017 [arXiv:2305.05710] [INSPIRE].

[48] J. Bijnens and M. Maul, *Large extra dimensions in rare decays*, *JHEP* **10** (2000) 003 [hep-ph/0006042] [INSPIRE].

[49] G. Degrassi, E. Gabrielli and L. Trentadue, *Flavor Changing Fermion-Graviton Vertices*, *Phys. Rev. D* **79** (2009) 053004 [arXiv:0812.3262] [INSPIRE].

[50] A. Blondel et al., *Searches for long-lived particles at the future FCC-ee*, *Front. in Phys.* **10** (2022) 967881 [arXiv:2203.05502] [INSPIRE].

[51] M. Drewes, *Distinguishing Dirac and Majorana Heavy Neutrinos at Lepton Colliders*, *PoS* **ICHEP2022** (2022) 608 [arXiv:2210.17110] [INSPIRE].

[52] M. Ovchynnikov and J.-Y. Zhu, *Search for the dipole portal of heavy neutral leptons at future colliders*, *JHEP* **07** (2023) 039 [arXiv:2301.08592] [INSPIRE].

[53] J.F. Nieves and P.B. Pal, *Gravitational decay of the Z-boson*, *Phys. Rev. D* **72** (2005) 093006 [hep-ph/0509321] [INSPIRE].

[54] B.C. Allanach, J.P. Skittrall and K. Sridhar, *Z boson decay to photon plus Kaluza-Klein graviton in large extra dimensions*, *JHEP* **11** (2007) 089 [arXiv:0705.1953] [INSPIRE].

[55] M. Kawasaki, K. Kohri and T. Moroi, *Big-Bang nucleosynthesis and hadronic decay of long-lived massive particles*, *Phys. Rev. D* **71** (2005) 083502 [astro-ph/0408426] [INSPIRE].

[56] M. Casse, J. Paul, G. Bertone and G. Sigl, *Gamma-rays from the galactic bulge and large extra dimensions*, *Phys. Rev. Lett.* **92** (2004) 111102 [hep-ph/0309173] [INSPIRE].

[57] N. Ishizuka and M. Yoshimura, *Axion and Dilaton Emissivity From Nascent Neutron Stars*, *Prog. Theor. Phys.* **84** (1990) 233 [INSPIRE].

[58] P.S.B. Dev, R.N. Mohapatra and Y. Zhang, *Revisiting supernova constraints on a light CP-even scalar*, *JCAP* **08** (2020) 003 [*Erratum ibid.* **11** (2020) E01] [arXiv:2005.00490] [INSPIRE].

JHEP01(2026)019

[59] M.B. Larson and B. Link, *Superfluid friction and late-time thermal evolution of neutron stars*, *Astrophys. J.* **521** (1999) 271 [astro-ph/9810441] [INSPIRE].

[60] A.V. Kisselev and V.A. Petrov, *Gravireggeons and transplanckian scattering in models with one extra dimension*, *Phys. Rev. D* **71** (2005) 124032 [hep-ph/0504203] [INSPIRE].

[61] P. Cox and T. Gherghetta, *Radion Dynamics and Phenomenology in the Linear Dilaton Model*, *JHEP* **05** (2012) 149 [arXiv:1203.5870] [INSPIRE].

[62] ATLAS collaboration, *Search for periodic signals in the dielectron and diphoton invariant mass spectra using* $139\,fb^{-1}$ *of pp collisions at* $\sqrt{s} = 13$ *TeV with the ATLAS detector*, *JHEP* **10** (2023) 079 [arXiv:2305.10894] [INSPIRE].

[63] J. Blumlein et al., *Limits on neutral light scalar and pseudoscalar particles in a proton beam dump experiment*, *Z. Phys. C* **51** (1991) 341 [INSPIRE].

[64] J.D. Bjorken et al., *Search for Neutral Metastable Penetrating Particles Produced in the SLAC Beam Dump*, *Phys. Rev. D* **38** (1988) 3375 [INSPIRE].

[65] A. de Giorgi and S. Vogl, *Dark matter interacting via a massive spin-2 mediator in warped extra-dimensions*, *JHEP* **11** (2021) 036 [arXiv:2105.06794] [INSPIRE].

[66] R.S. Chivukula et al., *Limits on Kaluza-Klein portal dark matter models*, *Phys. Rev. D* **111** (2025) 075030 [arXiv:2411.02509] [INSPIRE].

[67] H.M. Lee, M. Park and V. Sanz, *Gravity-mediated (or Composite) Dark Matter*, *Eur. Phys. J. C* **74** (2014) 2715 [arXiv:1306.4107] [INSPIRE].

[68] S. Hannestad and G. Raffelt, *New supernova limit on large extra dimensions*, *Phys. Rev. Lett.* **87** (2001) 051301 [hep-ph/0103201] [INSPIRE].

[69] S. Hannestad and G.G. Raffelt, *Stringent neutron star limits on large extra dimensions*, *Phys. Rev. Lett.* **88** (2002) 071301 [hep-ph/0110067] [INSPIRE].

[70] Particle Data Group collaboration, *Review of Particle Physics*, *PTEP* **2022** (2022) 083C01 [INSPIRE].

JHEP01(2026)019